國立臺灣大學醫學院免疫學研究所

碩士論文

Graduate Institute of Immunology

College of Medicine

National Taiwan University

Master Thesis

表現無唾液酸神經節苷脂之肝臟駐留記憶性 T 細胞對原發性膽汁性膽管炎參與角色之研究

The Role of Asialo-GM1^{+} Liver Resident Memory T cells in Primary Biliary Cholangitis

廖至宣

Chih-Hsuan Liao

指導教授：許秉寧 博士

Advisor: Ping-Ning Hsu, Ph.D.

中華民國一一一年七月

July, 2022

doi:10.6342/NTU202202017

國立臺灣大學碩士學位論文
口試委員會審定書
MASTER'S THESIS ACCEPTANCE CERTIFICATE
NATIONAL TAIWAN UNIVERSITY

表現無唾液酸神經節苷脂之肝臟駐留記憶性 T 細胞
對原發性膽汁性膽管炎參與角色之研究

The Role of Asialo-GM1^{+} Liver Resident Memory T cells
in Primary Biliary Cholangitis

本論文係廖至宣（學號 R09449011）在國立臺灣大學醫學院免疫學研究所完成之碩士學位論文，於民國 111 年 7 月 29 日承下列考試委員審查通過及口試及格，特此證明。

The undersigned, appointed by the Graduate Institute of Immunology, College of Medicine on July 29th, 2022 have examined a Master's thesis entitled above presented by Chih-Husan Liao (student ID: R09449011) candidate and hereby certify that it is worthy of acceptance.

口試委員 Oral examination committee:

（指導教授 Advisor）

系主任/所長 Director: 鄧述諄

doi:10.6342/NTU202202017

誌謝

轉眼間兩年的時光就過去了，即將要迎來尾聲，一路上遇到許多的人事物，我都懷著感恩的心看待一切。首先最感謝的是許秉寧老師，還記得剛進入免疫所的我懵懵懂懂，在與老師討論未來研究規劃時，感謝老師二話不說便答應指導我，讓我踏入肝臟科學這個領域，也感謝在老師嚴謹的指導下，讓我的研究能有更好的邏輯與結果。雖然每週的進度報告彷彿在不斷追趕著我，使我們得絞盡腦汁思考接下來的實驗規劃，但也因有著這些訓練的過程，使我能在短短的兩年能有一定的實驗成果，真的令我收穫良多。

在 R511 這個大家庭中，每個人都非常的照顧我。謝謝 Chris 學長在我剛進來時給我許多實驗上的建議，也常常買好多好吃的東西給大家吃，希望學長在美國能一切順利。謝謝華翊學長在我的研究中，無論是邏輯上、數據呈現上、以及操作細節上都給我莫大的幫助；謝謝思傑學長，沒聽到你的口頭禪或口哨聲總是覺得有些不習慣，也很能活絡實驗室的氣氛；謝謝世鐸學長，總是親手做好吃的甜點給大家吃，也分享很多有趣的知識。也要謝謝夢珣學姊、玉娟學姊、侑靜、宇軒、新加入的琳憑，還有 R508 的森強、怡怡和岡軒，感謝有你們一起陪伴著我成長，讓我在實驗室的時光總是過得開心且充實。

謝謝免疫所各位老師的指導，在 Seminar 課程中大家一起腦力激盪，討論許多實驗的細節與數據；下課後或是實驗間的空檔和同學們一起吃飯聊天講八卦甚至是很難笑的冷笑話，或許未來我會很懷念這些點點滴滴。

最重要的，要謝謝我的家人們，總是做我最強大的後盾，支撐著我完成這兩年的學業，讓我可以無後顧之憂的專心在學業上，也支持我做我喜歡的事和每個決定，期望我能更有一番成就，能夠成為你們的驕傲。也要感謝我的女朋友，從大學到研究所陪伴了我六年，歷經所有酸甜苦辣都有妳在，一起在這些時光中成長，為了彼此成為更好的自己。

最後，感謝我自己，遇到問題沒有放棄，而是抬起頭來面對並努力解決，儘管自己不是最優秀的那個人，但只求不愧對自己，期許未來在面對更多挑戰時，也能不忘初衷，相信命運的安排。

廖至宣 筆

doi:10.6342/NTU202202017

中文摘要

原發性膽汁性膽管炎(Primary Biliary Cholangitis, PBC)是一種自體免疫肝臟疾病，其特徵為在病患體內產生針對粒線體自體抗原的自體抗體。誘發 PBC 的機制有非常多因素，然而肝臟內 T 細胞所誘發的免疫反應在此疾病下仍然未知。在所有 T 細胞族群之中，組織駐留記憶性 T 細胞(Tissue Resident Memory, T_{RM})是一群具備停留與維持於特定組織中的能力而得名的細胞。在本實驗室的先前研究中發現有一群特定表現無唾液酸神經節苷脂(ASGM1)的 CD8 T 細胞存在於小鼠肝臟中，並與其他文獻記載之肝臟駐留記憶性 T 細胞具備相似特性。我們發現這群細胞在 B 型肝炎高壓注射轉染模式中對於病毒清除非常重要。此外，在刀豆蛋白 A 引發之急性肝炎模式中也發現這群細胞會於早期快速產生 IFN-γ 並引發急性肝炎。為了更進一步剖析這群細胞，於此論文中我們利用 2-辛炔酸-卵白蛋白(2-octynoic acid-ovalbumin, 2-OA-OVA)所誘發的自體免疫膽管炎動物模式用以模擬人體的原發性膽汁性膽管炎來探討這群細胞的角色。我們發現在誘發自體免疫膽管炎的野生型小鼠與缺乏先天性淋巴細胞的 $NFIL3^{-/-}$小鼠給予 anti-ASGM1 剔除性抗體都可以觀察到膽管炎有效被抑制，證明其為透過非自然殺手細胞(nature killer cell, NK cell)誘導的機制。我們以另一種得以剔除 T_{RM} 的 anti-CXCR3 抗體以剔除細胞，亦可以觀察到小鼠的膽管炎被抑制。我們進一步以質譜流式細胞術進行分析並發現 ASGM1 陽性 CD8 T 細胞為主要干擾素 γ (IFN-γ)來源並可能導致自體免疫膽管炎的產生。透過免疫組織化學染色可以觀察到給予 anti-ASGM1 和 anti-CXCR3 抗體都能抑制肝臟中 IFN-γ 的堆積。此外，在以 anti-ASGM1 消耗細胞後利用 α-半乳糖神經醯胺(α-galactosylceramide, α-GalCer)刺激 NKT 細胞後，血清中 IFN-γ 濃度明顯降低。將 α-Galcer 刺激活化之 NKT 細胞與 ASGM1 陽性肝臟駐留 CD8 T 細胞共培養後觀察到產生 IFN-γ 之細胞數明顯較多。綜上所述，ASGM1 陽性肝臟駐留 CD8 T 細胞在自體免疫膽管炎模式中是 IFN-γ 的主要來源，並對於膽管炎的發展扮演重要的角色。

doi:10.6342/NTU202202017

關鍵字：自體免疫性膽管炎、2-辛炔酸-卵白蛋白、組織駐留記憶性 T 細胞、無唾液酸神經節苷脂、CD8 T 細胞、干擾素 γ、質譜流式細胞術

doi:10.6342/NTU202202017

Abstract

Primary biliary cholangitis (PBC) is an autoimmune liver disease characterized by specific anti-mitochondrial antibodies (AMAs) targeted at mitochondrial autoantigens. The pathophysiology of PBC is multifactorial, whereas the detailed immune response triggered by the intrahepatic T lymphocytes still remains unknown. Among all T cell subsets, tissue-resident memory T cell (T_{RM}) is a specific lineage of lymphocytes, given its name by the ability to reside and maintain in different tissues. In our previous study, we identified a distinct Asialo-GM1-positive ($ASGM1^{+}$) CD8 T cell population in intrahepatic lymphocytes (IHLs) and exhibited similar properties with the previously reported liver-resident memory T cells. In the hepatitis B virus (HBV) hydrodynamic transfection model, we found that this population is crucial for the eradication of HBV. Moreover, this population was also identified as an early IFN-γ producer and critical for the initiation of the ConA-induced acute hepatitis model. To further dissect this specific population within this work, the role of $ASGM1^{+}$ liver T_{RM} cells was investigated in autoimmune cholangitis with 2-octynoic acid-ovalbumin (2-OA-OVA) immunization mouse model, comparing to the PBC disease in human bodies. We found that autoimmune cholangitis was suppressed by α-ASGM1 treatment through an NK cell-independent mechanism, with similar results shown by utilizing $NFIL3^{-/-}$ mice. We also applied an alternative way for liver T_{RM} depletion by the α-CXCR3 treatment, which was also found

doi:10.6342/NTU202202017

capable of suppressing autoimmune cholangitis. Moreover, through Mass Cytometry (CyTOF) analysis, we found that ASGM1$^+$ CD8 T cells were the main source of IFN-γ and might be responsible for the pathogenesis of autoimmune cholangitis. By immunohistochemical staining, we demonstrated that α-ASGM1 and α-CXCR3 treatment suppressed IFN-γ deposition in portal tracts. When mice were pre-treated with α-ASGM1 followed by α-galactosylceramide (α-GalCer) exposure, the serum level of IFN-γ was significantly suppressed but not IL-4. Further, when co-cultured with α-GalCer-stimulated NKT cells, we identified that ASGM1$^+$ liver T_{RM} cells were activated upon iNKT activation and contributed to IFN-γ production. Taken together, it was suggested that the ASGM1$^+$ CD8 liver T_{RM} cells were crucial for the development of 2-OA-OVA immunized autoimmune cholangitis and served as a source of IFN-γ deposition.

Key words: Primary biliary cholangitis; 2-octynoic acid; Tissue resident memory T cell; Asialo-GM1; CD8 T cell; Interferon-γ; Mass Cytometry (CyTOF)

doi:10.6342/NTU202202017

Contents

doi:10.6342/NTU202202017

doi:10.6342/NTU202202017

List of Figures

doi:10.6342/NTU202202017

Chapter 1 Introduction

1. Synopses of structure and fundamental functions of the liver

The liver is a reddish-brown, wedge-shaped organ positioned in the right upper quadrant of the abdominal cavity, and lobules are the functional units of the liver. By connecting to the hepatic artery and portal vein, the liver handles oxygenated blood supply from the aorta and delivery of blood containing digested nutrients from the gastrointestinal tract. The liver processes several important physiological functions, including detoxification, bile acid production, storage of fat-soluble vitamins, glycogenesis, breakdown of red blood cells, and production of hormones. Moreover, The liver is the only internal organ with the ability of natural regeneration. However, the liver is still vulnerable to a person with poor diet and lifestyle practices.

The liver serves as the human frontline immune system, constantly exposed and designed to recognize, trap, and eliminate bacteria, viruses, and macromolecules. Therefore, the liver must achieve a delicate balance between immune tolerance and immune surveillance against malignancy or infections. Several subsets of immune cells are present within the liver. As for myeloid cell subsets, Kupffer cells (KC) constitute the largest portion located in the liver. When localized to the liver, KCs reside primarily in the sinusoidal vascular space of the periportal region [1] and appear to remove endotoxins from the bloodstream and clear debris and microbes by phagocytosis. It also plays an

doi:10.6342/NTU202202017

important role in liver progenitor cell proliferation [2]. In addition, KCs and myeloid-derived suppressor cells (MDSCs) constitutively express IL-10 and TNF-β, providing a cytokine microenvironment unique to uninfected livers, rendering resident DCs tolerogenic and moderate T cell responses [3].

As the counterparts of myeloid cells, lymphocyte subpopulations of the innate and adaptive immune system are found scattered throughout the liver parenchyma. The liver is selectively enriched for key components of the innate immune system: mucosa-associated invariant T cells (MAIT), natural killer cells (NK), natural killer T cells (NKT), and γδ T cells. In particular, NK and NKT cells are important for producing cytokines to regulate both innate and adaptive immunity [4-7]. Adaptive cell populations are also present in the liver, such as CD4 T cells, CD8 T cells, and B cells. In addition, CD8 T cells, activated T cells, and memory T cells are particularly abundant for the eradication and sequestration of invading pathogens in the liver [8].

Canonical programming of immune tolerance in the liver prevents unwanted inflammatory responses to harmless food antigens or normal microbes. Hence, we need to study the balanced immune response within the liver.

2. Tissue-resident memory cells (T_{RM})

Tissue-resident memory T cells (T_{RM}) are a specific lineage of lymphocytes that are

doi:10.6342/NTU202202017

distinguished by their phenotype and function from peripheral central memory (T_{CM}) or effector memory (T_{EM}) T cells, with the ability to reside in a tissue or organ, providing frontline defense against infections and accelerate the clearance of pathogens. Many subsets of tissue-resident lymphocytes expressed CD44, CD69, CD49a, and CD103. In addition, the absence of CD62L and CCR7 suggested that these cells do not recirculate into lymphoid tissues and may persist in the tissues and organs [9,10].

2.1. Liver-resident memory T cells

Tissue-resident memory T cells discriminated themselves from their circulating counterparts by the expression of tissue residence-related markers and transcriptional regulation [11]. Liver-resident memory T cells are distinct from other T_{RM} cells, whose CD103 was not upregulated in mouse [12]. In addition, liver-resident CD8 T cells used a different way to reside in livers compared with T_{RM} cells in other tissues. Liver sinusoidal endothelium formed a porous structure, providing an ideal pattern for T cell patrolling and monitoring intrahepatic infections. Sinusoidal T cells were capable of interacting with hepatocytes due to the close association between sinusoids and hepatocytes [13,14].

A previous study reported that liver CD8 T_{RM} cells expressed CD69 and LFA-1 and patrolled hepatic sinusoids by interacting with ICAM-1 [15]. Moreover, liver CD8 T_{RM} cells expressed chemokine receptors CXCR3 and CXCR6 to maintain their retention in the liver. Transcription factors like HOBIT and BLIMP1 were also important for liver T_{RM}

doi:10.6342/NTU202202017

cells, which downregulated molecules associated with tissue egress and suppressed T_{CM} development [16]. In addition, liver T_{RM} cells played an important role in pathogen clearance. The combining of hepatitis and priming dendritic cells with hepatocyte-related antigens can induce a large amount of T_{RM} cells, which play an important role in defending against malarial sporozoite challenge [12].

In our previous study, we identified a specific Asialo-GM1 (ASGM1)-positive CD8 T cell population within intrahepatic lymphocytes of unimmunized mice, which shared similar characteristics with previously reported liver T_{RM} cells. [17]. ASGM1 is a glycosphingolipid derived from hydrolyzing the α-2,3 linkage on GM1 by β-1,4-N-acetylgalactosaminyl-transferase 1 (B4GALNT1), which is also involved in upregulating *o*-series gangliosides expression [18]. ASGM1 was used for NK cell identification [19]. However, NFIL3-KO mice, which are deficient in innate lymphoid cells (ILCs) and NK cells, treated with anti-ASGM1 antisera completely abrogated hepatitis B virus (HBV) eradication ability. In addition, intrahepatic $ASGM1^+$ CD8 T cells shared a similar phenotype with hepatic T_{RM} cells by expressing CD44, CD69, and LFA-1. ASGM1 has also been suggested to act as a liver immune cell marker. Despite their important role in defending against HBV, the in-depth immune responses induced by $ASGM1^+$ CD8 T cells in the liver required further investigation.

doi:10.6342/NTU202202017

3. Autoimmune hepatitis (AIH)

Hepatitis is a form of inflammation that occurs in the liver and can be caused by a variety of viruses or noninfectious agents, contributing to a wide range of disorders and death. Viral hepatitis is the most common type caused by one of several hepatitis viruses, whereas autoimmune hepatitis (AIH) is a chronic, self-perpetuating inflammatory disease resulting from loss of resistance, which can lead to cirrhosis, liver cancer, or death [20]. AIH is characterized by elevated immunoglobulin G and/or detection of characteristic autoantibodies, and typical patterns in liver histology [21]. AIH is a global disease that affects children and adults of all ethnicities and races. Diagnosis of AIH requires the exclusion of other causes and responses to immunosuppressive therapy. AIH can be classified into two types. Type 1 AIH is positive for autoantibodies targeting nuclear (ANA) and/or smooth muscle (SMA) self-antigens, and type 2 AIH is positive for anti-liver-renal microsomal antibody type 1 (anti-LKM1), type 3 (anti-LKM3) and/or anti-liver cytosolic type 1 (anti-LC1) antibodies [22].

Current studies estimate the annual new cases (incidence rate) to be 1-2 per 100,000 and the total cases (prevalence) to be approximately 24 per 100,000. Clinical manifestations and outcomes vary by geographic region, ethnicity, and race, even within the same country. In 2019, a very comprehensive practice guide and guidelines for AIH were published. In first-line treatments, corticosteroids alone or in combination with

doi:10.6342/NTU202202017

corticosteroids and azathioprine (AZA) have been shown to improve outcomes in patients with AIH [23]. However, complete discontinuation of therapy has been achieved only in a minority of AIH patients. Nevertheless, the mechanisms of AIH development required for deeper investigation remain unclear.

4. Primary biliary cholangitis (PBC)

Primary biliary cholangitis (PBC), formerly known as primary biliary cirrhosis, is an autoimmune liver disease characterized by specific anti-mitochondrial antibodies (AMAs) against mitochondrial autoantigens [24]. PBC is occurred predominantly in females, with a 1:9 male-to-female ratio. The highest prevalence rates were found in China, the United States, and the United Kingdom (49.2, 40.2, and 24.0 per 100,000 persons, respectively), while Canada and Australia had the lowest prevalence (2.2 and 1.9, respectively). The pathophysiology of PBC is multifactorial. However, loss of immune tolerance to biliary epithelial cells (BECs) is primarily involved and consequently leads to, cholestasis, liver fibrosis, and ultimately cirrhosis. The clinical manifestation of PBC ranged from asymptomatic cholestasis to cholestatic pruritus and severe end-stage biliary cirrhosis. The presence of serum AMA targeting the E2 subunit of the pyruvate dehydrogenase complex (PDC-E2) was the main characteristic of PBC (>95% of patients). In addition, antinuclear antibodies (ANA) directed against the nuclear autoantigen Sp100

doi:10.6342/NTU202202017

(anti-sp100) and 210-kDa glycoprotein (anti-gp210) are specifically used for confirming the diagnosis of PBC [25]. Ursodeoxycholic acid (UDCA) is a first-line therapy approved by the US Food and Drug Administration (FDA) for the treatment of PBC. Patients exhibited slower PBC progression, improved cholestasis serum biochemical parameters, and liver histology through long-term administration of UDCA. Nevertheless, symptoms such as fatigue and pruritus were not significantly improved by UDCA, and up to 40% of PBC patients have an incomplete response to UDCA treatment. For patients with poor response or intolerance to UDCA, a synthetic bile acid derivative named obeticholic acid (OCA), which potently activates the nuclear farnesoid X receptor (FXR), was administered as a monotherapy or combined with UDCA [24,26]. However, the safety and tolerability of OCA treatment should be monitored since it was associated with the development or exacerbation of pruritus. The etiology and pathogenesis of PBC remain uncertain despite intensive studies that have demonstrated the complexity of both innate and adaptive immune responses.

4.1. Xenobiotic-induced murine autoimmune cholangitis

Since multiple factors appear to be involved in the development of PBC, its clinical course can be complicated. Therefore, it is of value to elucidate the pathogenesis of PBC using animal models. Not only genetic factors but also environmental factors have been suggested to participate in PBC progression. Compromised resistance to PDC-E2 is

doi:10.6342/NTU202202017

believed to be the initial step in PBC pathology. This hypothesis was successfully validated by analyzing a large panel of chemicals by quantitative structure-activity relationship studies for reactivity to anti-PDC-E2 autoantibodies and the requirement for the structural integrity of the PDC-E2 lipoyl domain in AMA detection [27,28]. Exposure to xenobiotics induced autoimmune cholangitis by the failure of immune tolerance and implicated environmental factors in the pathogenesis of PBC [29].

As a commonly used cosmetic ingredient or flavoring agent in general foods, 2-octynoic acid (2-OA) is a xenobiotic compound with AMA affinity higher than PDC-E2 autoantigen. In a previous study, Wakabayashi et al. immunized female C57BL/6 mice with 2-OA conjugated to BSA and developed AMA as early as 4 weeks after immunization and maintained positive thereafter [30]. Pro-inflammatory like IFN-γ and TNF-α were also increased in serum at 4 weeks after immunization. These mice exhibited several symptoms including lymphocytic infiltration, bile duct damage, and granuloma formation 12 weeks after immunization. Immunostaining exhibited that there were mainly CD4 and CD8 T cell infiltration in the portal area, with the latter being more prevalent.

The role of innate immune effector cells in regulating disease activity, such as natural killer (NK) cells and NKT cells, was considered in this hypothesis-based model that initial events during immunization play an important role in disrupting tolerance [31]. Thus,

doi:10.6342/NTU202202017

further studies have been reported in which 2-OA-BSA immunized with and without the addition of the iNKT cell activator α-galactosylceramide (α-GalCer) were followed for AMA and liver pathology. 2-OA-BSA immunized mice exposed to α-GalCer developed more severe exacerbations of their autoimmune cholangitis. More interestingly, these mice produced increased levels of AMAs and have shown evidence of fibrosis [32].

5. Rationale and specific aims

Previous studies have been well investigated into the role of liver-resident memory T cells in mouse models of infections or diseases. ASGM1$^+$ CD8 liver T_{RM} cells formed a distinct subset and were more likely to activate and produce pro-inflammatory cytokines in the liver. Our previous study showed that the reduced vial clearance of HBV and IFN-γ-producing cells in HBV-specific ELISpot assay was found in the HBV transfection model through depletion of ASGM1$^+$ CD8 liver T_{RM} cells. Moreover, this population was also identified as an early IFN-γ producer and critical for the initiation of the ConA-induced acute hepatitis model. However, how these specific cell subsets of the liver participate in regulating autoimmune or tumor models is still undiscovered. Thus, we discussed the role of ASGM1$^+$ CD8 liver T_{RM} cells in the chronic 2-OA-OVA immunized primary biliary cholangitis (PBC) model to imitate the human PBC disorder. This study has three major goals: (1) Identify the distinct CD8 T cell subset of the phenotype and

doi:10.6342/NTU202202017

functions to explore their differences from other tissue-resident memory T cells; (2) Observe the pathogenicity in the 2-OA-OVA immunized PBC in WT and NFIL3 KO mice by depletion of the intrahepatic T_{RM} cells. We also used α-CXCR3 treatment to alternatively deplete this population and monitor the symptoms of 2-OA-OVA-immunized PBC to clarify the contribution of this population; (3) Identify the pathogenic role of ASGM1^{+} CD8 liver T_{RM} cells by their function or interaction under 2-OA-OVA immunized PBC.

doi:10.6342/NTU202202017

Chapter 2 Materials and Methods

1. Materials

1.1. Mice

Female wild-type (WT) C57BL/6 mice aged 8-10 weeks used in this study were purchased from the National Taiwan University Animal Center and the National Laboratory Animal Center (Taipei, Taiwan). Genetic knock-out of nuclear factor, interleukin 3 regulated (NFIL3 KO) mice on the C57BL/6 background were generously provided by Dr. Tak W. Mak (Department of Immunology, University of Toronto). All mice were kept in the specific pathogen-free (SPF) facility in the Animal Center of the College of Medicine, National Taiwan University. All the experimental procedures and the use of the animals were reviewed and approved by the Institutional Animal Care and Use Committee (IACUC) of the National Taiwan University College of Medicine and College of Public Health.

1.2. Kits

Fixation/Permeabilization kit	Invitrogen (Carlsbad, CA, USA)
MojoSort^{TM} Mouse CD3^{+} T cell Isolation Kit	BioLegend (San Diego, CA, USA)
Mouse IFN-γ ELISA kit	BioLegend (San Diego, CA, USA)

doi:10.6342/NTU202202017

Mouse TNF-α ELISA kit	BioLegend (San Diego, CA, USA)
Mouse IL-4 ELISA kit	BioLegend (San Diego, CA, USA)
iScript™ cDNA Synthesis Kit	Bio-Rad (Hercules, CA, USA)

1.3. Antibodies

Anti-asialo GM1 (Rabbit)	Invitrogen (Carlsbad, CA, USA)
Anti-Asialo-GM1 Alexa Flour®647 (clone: Poly21460)	BioLegend (San Diego, CA, USA)
Anti-mouse CD3 BV421 (clone: 17A2)	BioLegend (San Diego, CA, USA)
Anti-mouse CD3 FITC (clone: 17A2)	BioLegend (San Diego, CA, USA)
Anti-mouse CD4 BV510 (clone: RM4-5)	BioLegend (San Diego, CA, USA)
Anti-mouse CD4 APC-Cy7 (clone: RM4-5)	BioLegend (San Diego, CA, USA)
Anti-mouse CD8α BV510 (clone: 53-6.7)	BioLegend (San Diego, CA, USA)
Anti-mouse CD8α PE-Cy7 (clone: 53-6.7)	BioLegend (San Diego, CA, USA)
Anti-mouse CD11a (LFA-1) PerCP-Cy5.5 (clone: M17/4)	BioLegend (San Diego, CA, USA)

doi:10.6342/NTU202202017

Anti-mouse CD44 APC (clone: IM7)	BioLegend (San Diego, CA, USA)
Anti-mouse CD44 APC-Cy7 (clone: IM7)	BioLegend (San Diego, CA, USA)
Anti-mouse CD49b (DX5) PE (clone: HMα2)	BioLegend (San Diego, CA, USA)
Anti-mouse CD62L FITC (clone: MEL-14)	BioLegend (San Diego, CA, USA)
Anti-mouse CD69 FITC (clone: H1.2F3)	BioLegend (San Diego, CA, USA)
Anti-mouse CD103 PerCP-Cy5.5 (clone: M290)	BioLegend (San Diego, CA, USA)
Anti-mouse CXCR3 APC-Cy7 (clone: CXCR3-173)	BioLegend (San Diego, CA, USA)
Anti-mouse IFN-γ PE (clone: XMG1.2)	BioLegend (San Diego, CA, USA)
Anti-mouse NK1.1 BV510 (clone: PK136)	BioLegend (San Diego, CA, USA)
HRP-conjugated goat anti-mouse IgG	Invitrogen (Carlsbad, CA, USA)
HRP-conjugated goat anti-mouse IgM	Invitrogen (Carlsbad, CA, USA)
LEAF™ purified anti-human CD3 (clone: OKT3)	BioLegend (San Diego, CA, USA)
LEAF™ purified anti-mouse CD3ε (clone: BM10-37)	BioLegend (San Diego, CA, USA)
LEAF™ purified anti-mouse CD28	BioLegend (San Diego, CA, USA)

doi:10.6342/NTU202202017

(clone: CD28.2)

LEAF™ purified anti-human CD28 (clone: 37.51) — BioLegend (San Diego, CA, USA)

Ultra-LEAFTM Purified anti-Asialo-GM1 Antibody (clone: Poly21460) — BioLegend (San Diego, CA, USA)

Ultra-LEAF™ Purified anti-mouse CD183 (CXCR3, clone: 173) — BioLegend (San Diego, CA, USA)

1.4. Chemicals and reagents

2-octynoic acid-ovalbumin (2-OA-OVA)	LTK BioLaboratories (Taoyuan, Taiwan)
α-galactosylceramide (α-GalCer, KRN7000)	Cayman Chemical (Ann Arbor, MI, USA)
Ampicillin	MD Biotech (Morgantown, WV, USA)
Carboxyfluorescein succinimidyl ester (CFSE)	Invitrogen (Waltham, MA, USA)
Complete Freund's adjuvant (CFA)	Sigma Aldrich (St. Louis, MO, USA)
Collagenase from *Clostridium histolyticum*	Sigma Aldrich (St. Louis, MO, USA)
Dimethyl sulfoxide (DMSO)	Merck KGaA (Darmstadt, Germany)

doi:10.6342/NTU202202017

Disodium hydrogen phosphate (Na_2HPO_4)	Merck KGaA (Darmstadt, Germany)
DNase I	Sigma Aldrich (St. Louis, MO, USA)
Ethylenediaminetetra-acetic acid (EDTA)	Sigma Aldrich (St. Louis, MO, USA)
Fetal bovine serum (FBS)	Corning (USA)
Ficoll-Paque PLUS	Cytiva (Marlborough, MA, USA)
Glucose	USB Corp. (Cleveland, Ohio, USA)
GlutaMAX™-1 (100X)	Gibco® (Carlsbad, CA, USA)
GolgiSTOP	BD Biosciences (San Diego, CA, USA)
Incomplete Freund's adjuvant (IFA)	Sigma Aldrich (St. Louis, MO, USA)
Ionomycin	Sigma Aldrich (St. Louis, MO, USA)
Methanol	Merck KGaA (Darmstadt, Germany)
Paraformaldehyde	New England Biolabs (Ipswich, MA, USA)
Percoll® PLUS	Cytiva (Marlborough, MA, USA)
Penicillin	Sigma Aldrich (St. Louis, MO, USA)
Phorbol 12-myristate 13-acetate (PMA)	Sigma Aldrich (St. Louis, MO, USA)
Potassium chloride (KCl)	Merck KGaA (Darmstadt, Germany)
Potassium dihydrogen phosphate	Merck KGaA (Darmstadt, Germany)

doi:10.6342/NTU202202017

(KH_2PO_4)	
Potassium hydrogen phosphate (K_2HPO_4)	Merck KGaA (Darmstadt, Germany)
Propidium iodine (PI)	Sigma Aldrich (St. Louis, MO, USA)
Protease inhibitor cocktail	Goal Bio (Taiwan)
RIPA buffer IV with Triton-X-100	Bio Basic Canada Inc.(Konrad Crescent,
(pH=7.4, 5X)	Markham ON, Canada)
RNase	Sigma Aldrich (St. Louis, MO, USA)
RPMI-1640 medium	Gibco® (Carlsbad, CA, USA)
Sodium bicarbonate ($NaHCO_3$)	Merck KGaA (Darmstadt, Germany)
Sodium chloride (NaCl)	USB Corp. (Cleveland, Ohio, USA)
Streptomycin	Sigma Aldrich (St. Louis, MO, USA)
Tetramethylbenzidine (TMB) substrate	R&D systems (Minneapolis, MN, USA)
Trypan Blue	Sigma Aldrich (St. Louis, MO, USA)
Trypsin-EDTA solution	Sigma Aldrich (St. Louis, MO, USA)
Tween 20	Sigma Aldrich (St. Louis, MO, USA)

1.5. Buffer

- 1% Casein

Dissolve 1 g Casein in 30 ml 0.3 M NaOH, stirring at 40℃, pH=7.5, then dissolve

doi:10.6342/NTU202202017

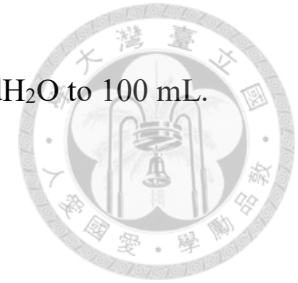

0.136 g KH_2PO_4 and 0.141 g Na_2HPO_4, stirring at 40℃, add ddH_2O to 100 mL.

- 2% Fluorescence-activated cell sorting (FACS) staining buffer

  2% v/v FBS/DPBS and a final concentration of EDTA 2 mM

- Collagenase IV digestion buffer

  20 mg of collagenase IV (Sigma-Aldrich) dissolved in 50 ml HBSS with Ca^{2+}, Mg^{2+}

- Dulbecco's PBS (DPBS), 10X stock

  Merck KGaA (Darmstadt, Germany)

- Fixation/Permeabilization buffer

  Dilute concentrate (1 part) into diluent (3 parts). 10X Permeabilization buffer was diluted with ddH_2O (Invitrogen, Waltham, MA, USA)

- Hank's Balanced Salt Solution (HBSS) with Calcium & Magnesium, 1X

  (Corning, USA)

- Hank's Balanced Salt Solution (HBSS) without Calcium, Magnesium, 1X

  (Corning, USA)

- Isotonic Percoll solution

  Combining Percoll™ with 10X DPBS. For working concentration, dilute the isotonic Percoll solution with 1X DPBS to make the required gradient.

- RBC lysis buffer (ACK buffer)

  8.29 g NH_4Cl

doi:10.6342/NTU202202017

7 ml 0.5 M EDTA

1 g $KHCO_3$

Dissolved in 1 L ddH_2O, pH=7.2

- RIPA lysis buffer

Diluting the 5X RIPA buffer with ddH_2O, 100X of protease inhibitor was added.

1.6. List of primers

Mouse β-actin	Forward	5’ CGTGCGTGACATCAAAGAGAA 3’
	Reverse	5’ TGGATGCCACAGGATTCCAT 3’
IFN-γ	Forward	5’ CAGCAACAGCAAGGCGAAAAAGG 3’
	Reverse	5’ TTTCCGCTTCCTGAGGCTGGAT 3’
Collagen-I	Forward	5’ ACGTCCTGGTGAAGTTGGTC 3’
	Reverse	5’ CAGGGAAGCCTCTTTCTCCT 3’
Collagen-III	Forward	5’ GTTCTAGAGGATGGCTGTACTAAACACA 3’
	Reverse	5’ TTGCCTTGCGTGTTTGATATTC 3’

1.7. Antibodies for CyTOF analysis

Antigen	Labeled Element	Mass	Species
CD45	Y	89	m
Granzyme B	Cd	114	m
TCRb	In	115	m

doi:10.6342/NTU202202017

Ly6G	La	139	m
CD11b	Ce	140	m
CD69	Pr	141	m
CD49b	Nd	142	m
CD11c	Nd	143	m
Gr1	Nd	144	m
CD4	Nd	145	m
CD3	Sm	147	m
CD103	Nd	148	m
Ly6C	Eu	151	m
Ki67	Sm	152	m, h
LFA-1	Sm	154	m
CD8a	Gd	155	m
CD107	Gd	156	m
CD49a	Gd	157	m
CXCR3	Gd	158	m
CXCR6	Tb	159	m
NK1.1	Gd	160	m
TCRgd	Dy	161	m
TNFa	Dy	162	m
CD62L	Dy	163	m
IFNg	Ho	165	m
Perforin	Er	166	m
Nkp46	Er	167	m
PD-1	Er	168	m
F4/80	Tm	169	m
CD49b	Er	170	m
CD44	Yb	171	m, h
AsialoGM1	Yb	172	
CD19	Yb	173	m

doi:10.6342/NTU202202017

IgM	Yb	174	m
CD127	Lu	175	m
CD45R/B220	Yb	176	m, h
MHCII	Bi	209	m

doi:10.6342/NTU202202017

2. Methods

2.1. Isolation of splenocytes (SPLs) and intrahepatic lymphocytes (IHLs)

To isolate splenocytes (SPLs), we first ground the spleens in PBS and filtered through a 40-μm strainer. After centrifugated for 400g, we lysed the red blood cells with ACK solution. For further experiment purpose, we used MojoSort^{TM} Mouse CD3 T cell Isolation Kit (BioLegend, USA) to enrich $CD3^+$ T cells from the SPL suspension.

To isolate intrahepatic lymphocytes (IHLs), we first perfused the livers with HBSS buffer (Corning, USA) and digested them with collagenase IV solution (Sigma-Aldrich, USA) immediately after sacrificing the mice. The shredded tissue were then suspended in HBSS buffer and ground with a plunger and passed through a 70-μm strainer. We centrifuged the suspension by 50g centrifugation for 5 minutes to remove hepatocytes and larger cell clumps. Next, we centrifuged the supernatant at 300g, 4℃ for 10 minutes to collect the pellet containing IHLs. Cells were resuspended in the gradient of 40%/70% isotonic Percoll (Cytiva, USA) solution and centrifuged at 1200g for 20 minutes without brake. The IHLs were collected from the interface in the centrifuged suspension, then washed by HBSS once.

2.2. Primary T cell culture

Primary T cells isolated from mice were cultured in RPMI-1640 medium (Gibco,

doi:10.6342/NTU202202017

USA) containing 10% FBS (Corning, USA), 1% Penicillin (Sigma-Aldrich, USA), 1% Streptomycin (Sigma-Aldrich), and 1% Ampicillin (MD Biotech, USA). After counting cell numbers by trypan blue exclusion. T cells were cultured in the 96-well flat-bottomed plate in the incubator under 37℃, 5% CO_2. For *ex vivo* T cell activation, T cells were cultured in the plates pre-coated with anti-CD3 (5 μg/ml) (BioLegend, USA) and the culture medium with soluble anti-CD28 (2 μg/ml) (BioLegend, USA).

2.3. Xenobiotic-induced primary biliary cholangitis model establishment

Female C57BL/6 or NFIL3 KO mice at 8-10 weeks of age were intraperitoneally immunized with 20 μg of 2-OA-OVA protein emulsified with complete Freund's adjuvant (CFA, Sigma-Aldrich, USA) and subsequently boosted at weeks 2, 4, 6 and 8 with 2-OA-OVA emulsified with incomplete Freund's adjuvant (IFA, Sigma-Aldrich, USA). At the first and second 2-OA-OVA immunizations, mice were also intravenously injected with 2 μg of α-galactosylceramide (α-GalCer).

2.4. *In vivo* depletion of intrahepatic lymphocytes (IHLs)

We utilized two types of antibody treatment, α-ASGM1 and α-CXCR3 antibodies, to deplete the distinct intrahepatic lymphocyte population. For the former one, we followed the instruction of the manufacturer to dissolve lyophilized anti-Asialo GM1

doi:10.6342/NTU202202017

(Wako, Japan) antibody in distilled water. Mice were intraperitoneally injected with 20 μl dissolved solution one day before 2-OA-OVA/α-GalCer immunization and further treated twice per week until sacrifice. For the latter treatment, mice were intravenously injected with 200 μg of α-CXCR3 antibody (BioLegend, USA) one day before 2-OA-OVA/α-GalCer immunization, and further treated with 100 μg of α-CXCR3 twice per week until sacrifice.

2.5. Histological examination

To analyze the pathological sections, we fixed the livers with 10% paraformaldehyde solution immediately after perfusion and kept 2-3 days at room temperature. The liver tissues were then embedded in paraffin and then cut into 4-μm sections for hematoxylin and eosin (H&E) staining and 5-μm sections for Masson's trichrome staining or immunohistochemical staining.

2.6. Determination of serum anti-PDC-E2 antibodies and cytokine levels

Submandibular blood was collected from mice at various time intervals between 2-OA-OVA/α-GalCer immunization. To analyze IgM and IgG autoantibodies, we first coated the ELISA plates with purified recombinant PDC-E2 at 1 μg/ml in carbonate buffer (pH 9.6) and preserved at 4°C overnight. After blocking with 1% casein for 1 hour,

doi:10.6342/NTU202202017

supernatants or diluted sera were added and incubated for 2 hours at room temperature. After washing the ELISA plates with PBS+0.5% Tween 20, horseradish peroxidase (HRP)-conjugated goat anti-mouse IgG (1:2000, Invitrogen, USA) and IgM (1:2000, Invitrogen, USA) were added into the plates. After 1-hour incubation, immunoreactivity was detected by measuring optical density (O.D.) at 450 nm after exposure to tetramethylbenzidine (TMB) substrate (R&D systems, Minneapolis, MN, USA) for 20 minutes. For pro-inflammatory cytokines, the serum levels of IFN-γ and TNF-α were conducted with ELISA kit, respectively (BioLegend, USA), followed by the standard protocols provided by the manufacturer.

2.7. Quantitative real-time PCR analysis

Total mRNA was extracted from mouse liver specimens by the TRI^{zol} method (Invitrogen Life Technologies, USA). For qPCR analysis, we converted extracted mRNA to complementary DNA (cDNA) according to the standard protocol of iScript™ cDNA Synthesis Kit (Bio-Rad, USA). Quantitative amplification was then detected by QuantStudio™ 3 Real-Time PCR System (Thermo Fisher Scientific, USA). The $2^{-\Delta\Delta Ct}$ was used to calculate the relative fold change of target genes.

2.8. Flow cytometric analysis of lymphocytes

doi:10.6342/NTU202202017

Splenocytes or intrahepatic lymphocytes were first suspended with FACS staining buffer (2% FBS in PBS with EDTA) and treated with the Fc receptor blocker (BD Biosciences, USA) for 10 minutes, followed by staining with surface marker-specific antibody for 30-60 minutes, 4℃. Overall, we labeled suspended cells with antibodies targeting CD3ε, CD4, CD8α, NK1.1, ASGM1, CD69, LFA-1, CXCR3, CD103, CD44, and CD62L (BioLegend, USA). After being washed twice with FACS staining buffer, cells were resuspended and analyzed by flow cytometer (Canto II, BD Biosciences, USA) and FlowJo™ Software (BD Biosciences, USA).

To analyze cytokine production, GolgiSTOP (BD Biosciences, USA) was applied 4 hours prior harvesting *ex vivo*-activated T cells. As for *in vivo* analysis, mice were intravenously injected with GolgiSTOP 1 hour prior to sacrifice. After stained with surface markers as mentioned above, cells were fixed with fixation buffer (Invitrogen, USA) at 4℃ for overnight. After permeabilized cell membrane by permeabilization buffer (Invitrogen, USA), IFN-γ staining was applied for 1 hour at room temperature. After cells were washed twice and resuspended in FACS staining buffer, we acquired cells with flow cytometer and analyzed with FlowJo™ Software as mentioned above.

2.9. Adoptive transfer

$CD45.2^+$ C57BL/6 mice were intravenously administered 1 μg of P2X7 inhibitor

doi:10.6342/NTU202202017

KN-62 (Cambridge, UK) to maintain the survival of intrahepatic lymphocytes [33]. After 30 minutes, we harvested IHLs and stained surface markers. $CD45.2^+$ CD8 T cells were then sorted into $ASGM1^+$/ $ASGM1^-$ populations We used FACSAria cell sorter (BD Biosciences, San Jose, CA) to purify $ASGM1^+$ and $ASGM1^-$ CD8 T cells. After verifying the viability of the sorted cells, around 2×10^5 $CD45.2^+$ donor cells were adoptively transferred into $CD45.1^+$ recipient mice through intravenous injection.

2.10. Single-cell mass cytometry (CyTOF)

We followed the sample preparation protocol from Dr. Shih-Yu Chen. First, we incubated the harvested IHLs with cisplatin for 1 minute at room temperature to verify the cell viability. After quenching cisplatin with RPMI + 10% FBS, we fixed cells by adding RPMI fixed buffer (RPMI + 1.5% paraformaldehyde) for 10 minutes at room temperature, followed by washing cells with CSM (PBS + 0.5% BSA). Palladium barcoding of fixed cell samples was conducted [34] followed by staining 34 surface markers with heavy metal-conjugated antibodies as described in the antibody list for 1 hour. Samples were then washed once with CSM, permeabilized on ice for 10 min, and incubated with heavy metal-conjugated antibodies against 5 intracellular markers for 1 hour. The cell samples were washed once with CSM and twice with water after intercalation/fixation. The detector sensitivity normalization was performed before mass

doi:10.6342/NTU202202017

measurement of samples [35]. After the measurement finished, files were debarcoded [34] and gated respectively.

2.11. Co-culture assay

Mice were i.v. injected with α-GalCer (2 μg/ml), and NKT cells were sorted out 4 hours post-injection. Naïve IHLs were also sorted into $ASGM1^{+}$/ $ASGM1^{-}$ CD8 T cells. Sorted cells were co-cultured with α-GalCer-stimulated NKT cells at a 1:1 ratio of 1.5×10^{5} cells for each for 24 hours in 96-well flat-bottomed plate, respectively. IFN-γ-producing CD8 T cells were determined by intracellular staining.

2.12. Statistical analysis

At least 3 representative experiments were performed and shown in mean ± SEM. Unpaired Student's t-tests were applied to determine the significance between the two experimental groups. Comparison of more than two groups was performed with one-way ANOVA followed by Tukey multiple comparison test. Data were analyzed by using GraphPad Prism 8.0.2 software (GraphPad Software, USA) and Microsoft Excel 2019 (Microsoft, USA). Statistically significant differences were defined as $*p < 0.05$, $**p < 0.01$, and $***p < 0.001$.

doi:10.6342/NTU202202017

Chapter 3 Results

1. A distinct ASGM1$^+$ CD8$^+$ T cell population persisted in the liver and exhibited phenotypic and functional liver T_{RM} characteristics.

According to our previous study, the intrahepatic lymphocytes (IHL) of the naïve mice consisted of distinct CD8 T cell population [17]. Sorting of the ASGM1$^+$ population revealed that the majority of IHL comprised CD3$^+$ T cells together with NK cells in the ASGM1$^+$ population of naïve mice **(Fig. 1A)**. However, there was no such population found in the peripheral control group. Furthermore, the ASGM1 expression was found particularly in the IHL CD8$^+$ T cell population **(Fig. 1B)**. These data indicated that there indeed existed a CD8$^+$ T cell population expressing ASGM1 in the IHLs.

We further used a panel of surface markers for tissue residence to analyze the phenotypic properties of the ASGM1$^+$ CD8 T cells in the IHL. Compared the total CD8 T cells in the IHLs with the lymphocytes collected from other tissues, we found that IHL expressed higher ASGM1, CD69, and LFA-1 than lymphocytes in peripheral or other tissues. However, since the liver-resident memory T cells (T_{RM}) were reported to lack CD103 expression [12], we showed that CD103 expression was not upregulated in IHL **(Fig. 1C)**. We next analyzed additional T_{RM} markers by comparing the ASGM1$^+$ CD8 T cells in IHLs to ASGM1$^-$ cells. The former showed a phenotype of CXCR3$^+$, CD69$^+$, LFA-1^{hi}, CD62L^{lo}, and CD44$^+$. CD103 was not upregulated, consistent with reported phenotypic

doi:10.6342/NTU202202017

characteristics of liver T_{RM} cells [12,15,16,37] **(Fig. 1D)**. We sorted out $ASGM1^+$/$ASGM1^-$ CD8 IHLs and adoptively transferred into recipient mice, and we found that only the $ASGM1^+$ CD8 T cells were able to settle and remain in the liver, whereas control $ASGM1^-$ and splenocytes were not **(Fig. 1E)**. Moreover, in our previous study, RNA microarray analysis discovered that liver $ASGM1^+$ CD8 T cells exhibited gene signature similar to the previously reported T_{RM} cells [17]. When $CD3^+$ IHLs and SPLs were harvested and cultured *ex vivo* under α-CD3/α-CD28 activation, the majority of IFN-γ-producing in the IHLs were $ASGM1^+$ CD8 T cells, whereas $ASGM1^-$ CD8 T cells were responsible in the SPLs **(Fig. 1F)**. Based on these results, we identified the specific $ASGM1^+$ CD8 T cells in IHLs sharing similar phenotype and functionality with liver T_{RM} cell population.

2. Autoimmune cholangitis and liver fibrosis were suppressed by α-ASGM1 treatment in 2-OA-OVA immunized autoimmune cholangitis.

Mice immunized with 2-OA-OVA would manifest autoimmune cholangitis, typical antimitochondrial antibodies (α-PDC-E2, AMA), an increase in $CD8^+$ liver infiltrating cells particularly co-expressed CD44, and with an elevation of serum IFN-γ and TNF-α. Furthermore, 2-OA-OVA immunized mice exposed to α-galactosylceramide (α-GalCer) developed a profound exacerbation of autoimmune cholangitis, including significant increases in $CD8^+$ T cell infiltrates, portal inflammation, granuloma formation, and bile

doi:10.6342/NTU202202017

duct damage [38,39]. To define the role of ASGM1$^+$ liver T_{RM} cells in the pathogenesis of autoimmune cholangitis, we first immunized wild-type (WT) C57BL/6 mice with 2-OA-OVA and α-GalCer exposure combined with or without α-ASGM1 treatment and monitored disease progress **(Fig. 2A)**. First, histological examination showed that α-ASGM1 treatment significantly decreased lymphocyte infiltration, portal inflammation and fibrosis **(Fig. 2B)**. These histological observations were supported by lower expression levels of IFN-γ, collagen I and collagen III fibrosis-related tissue mRNA in livers of α-ASGM1 treated mice compared to the untreated ones **(Fig. 2C)**. To confirm whether α-ASGM1 treatment was able to deplete liver T_{RM} population, we examined the reported liver T_{RM} surface marker expression. We noticed that there was a significant population that can be classified into LFA-1^{hi} CD69$^+$ population in intrahepatic CD8 T cells. Treated naïve mice with α-ASGM1 antibody significantly depleted LFA-1^{hi} CD69$^+$ subpopulation, with the phenotypic correspondence to the T_{RM} cells **(Fig. 2D)**. For serological analyses, anti-PDC-E2 IgM and IgG autoantibody titer were decreased in α-ASGM1-treated mice **(Fig. 2E)**. Serum levels of IFN-γ and TNF-α were also decreased in α-ASGM1-treated mice **(Fig. 2F)**. Moreover, liver-infiltrating lymphocyte subsets including total T, CD8 T, IFN-γ-producing T, B, NKT, and NK cells were all significantly decreased in α-ASGM1-treated mice **(Fig. 2G)**. These results demonstrated that the α-ASGM1 treatment significantly ameliorate 2-OA-OVA immunized autoimmune

doi:10.6342/NTU202202017

cholangitis, suggesting the specific ASGM1$^+$ CD8 T cell population participated in the progression of 2-OA-OVA immunized autoimmune cholangitis.

3. 2-OA-OVA immunized autoimmune cholangitis was suppressed by α-ASGM1 treatment through an NK cell-independent mechanism.

The previous study showed that natural killer cells (NK cells) were a major cell subset of ASGM1-positive cells in IHLs, and NK cells could be depleted by the anti-ASGM1 treatment [19]. Accordingly, NK cell populations were also significantly depleted in the livers of α-ASGM1-treated mice. To rule out the role of NK cells in autoimmune cholangitis, we utilized NFIL3$^{-/-}$ (KO) mice that are deficient in NK cells [40]. By sorting out liver ASGM1$^+$ cells from NFIL3-KO mice, we found that CD8 T cells instead of NK cells consisted of a large proportion in the ASGM1$^+$ cells **(Fig. 3A)**. After immunized NFIL3-KO mice with 2-OA-OVA, we found that the autoimmune cholangitis still progressed. However, histological examination showed that α-ASGM1 treatment significantly decreased lymphocyte infiltration, portal inflammation, and fibrosis **(Fig. 3B)**. Lower expression levels of IFN-γ, collagen I, and collagen III fibrosis-related tissue mRNA in livers of α-ASGM1-treated NFIL3 KO mice were still observed compared to the untreated ones **(Fig. 3C)**. In addition, anti-PDC-E2 autoantibody titer and IFN-γ and TNF-α production were also decreased in α-ASGM1-treated NFIL3 KO mice **(Fig. 3D-**

doi:10.6342/NTU202202017

3E). Moreover, liver-infiltrating lymphocyte subsets including total T, CD8 T, IFN-γ-producing T, B, and NKT cells but not NK cells were significantly decreased in α-ASGM1-treated mice **(Fig. 3F)**. The results suggested that the specific ASGM1$^+$ CD8 T_{RM} cells aside from NK cells in the IHLs played a crucial role in the progression of 2-OA-OVA immunized autoimmune cholangitis.

4. Depleting ASGM1$^+$ liver CD8$^+$ T cells through alternative α-CXCR3 treatment also suppressed autoimmune cholangitis and liver fibrosis.

Aside from NK cells, CD8 T consisted of a large proportion of the ASGM1$^+$ population in IHL. However, ASGM1 was expressed differently between all CD8 T cells. As shown in **Fig. 1D**, ASGM1$^+$ higher CXCR3 chemokine receptors were expressed by CD8 liver T_{RM} cells. The previous study has reported that α-CXCR3 administration could deplete the liver T_{RM} population [12], so we further turned to the α-CXCR3 treatment to investigate whether the protective effect was achieved in mice with 2-OA-OVA immunized autoimmune cholangitis as α-ASGM1 did **(Fig. 4A)**. We first examined the α-CXCR3 treatment on naïve mice and observed that both LFA-1^{hi} CD69$^+$ and LFA-1^{hi} CD44$^+$ population were significantly depleted **(Fig. 4B)**. Moreover, depletion of liver T_{RM} cells by α-CXCR3 treatment also decreased lymphocyte infiltration, portal inflammation and fibrosis in 2-OA-OVA immunized autoimmune cholangitis **(Fig. 4C)**. The

doi:10.6342/NTU202202017

expressions of IFN-γ, collagen I, and collagen III in α-CXCR3-treated mice were also significantly decreased corresponded to histological observations **(Fig. 4D)**. In addition, anti-PDC-E2 IgM and IgG were decreased in α-CXCR3 treated mice **(Fig. 4E)**. Serum IFN-γ and TNF-α were also decreased in α-CXCR3 treated mice **(Fig. 4F)**. Infiltrating lymphocyte subsets were significantly decreased except NK cells in α-CXCR3-treated mice **(Fig. 4G)**. We demonstrated that both α-ASGM1 and α-CXCR3 were able to deplete similar liver T_{RM} cell populations and reversed the 2-OA-OVA immunized autoimmune cholangitis, suggesting that the $ASGM1^+$ $CD8^+$ T cells with CXCR3 expression played an important role in the progression of 2-OA-OVA immunized autoimmune cholangitis.

5. IFN-γ was produced by activated $ASGM1^+$ liver $CD8^+$ T cells under 2-OA-OVA immunized autoimmune cholangitis.

For a deeper investigation, We utilized Mass Cytometry (CyTOF) to analyze the kinetics of different cell populations post-2-OA-OVA immunization. A staining panel containing 34 surface markers and 5 intracellular markers was performed to classify intrahepatic leukocytes. IHLs were collected at different time intervals after 2-OA-OVA immunization. With the differential expression of lineage-related markers, We divided IHLs into 11 clusters **(Fig. 5A)**. The overall dynamic changes of markers related to activation, resident, cytotoxic and effector functions for each subset at different time

doi:10.6342/NTU202202017

intervals under 2-OA-OVA immunized autoimmune cholangitis were shown **(Fig. 5B)**. Within all clusters, T cells and NKT cells exhibited high expression of IFN-γ and cytotoxicity molecules, whereas other subsets such as B cells, DCs and Kupffer cells were expanded along with the disease progression **(Fig. 5B-5C)**. We further compared differences in the IHL population with or without ant-ASGM1 treatment after 2-OA-OVA immunization. We interpreted the results of the CyTOF data and revealed that anti-ASGM1 treatment affected serum levels of IFN-γ in PBC mice. First, the major IFN-γ sources among 2-OA-OVA immunized autoimmune cholangitis were compared. We found that the anti-ASGM1 treatment mainly decreased the IFN-γ-producing CD8 T cell population. Subsequently, when mice were treated with anti-ASGM1, both IFN-γ-producing CD4 and CD8 T cells reduced in 5 weeks post-2-OA-OVA immunization **(Fig. 5D)**. Moreover, mice with autoimmune cholangitis received anti-ASGM1 treatment decreased the total IFN-γ expression level. Furthermore, we identified that $ASGM1^+$ $CD8^+$ T cells showed the highest mean fluorescence intensity (MFI) of IFN-γ **(Fig. 5E)**. However, $ASGM1^+$ $CD8^+$ T cells were not the major sources of other effector and cytotoxic molecules such as TNF-α, CD107a, perforin, and granzyme B. Also, these factors were not significantly affected by anti-ASGM1 treatment **(Fig. 5F-5I)**. Overall, these results indicated that the $ASGM1^+$ CD8 liver T_{RM} cells were the main source of hepatic IFN-γ to promote inflammatory responses in the 2-OA-OVA immunized

doi:10.6342/NTU202202017

autoimmune cholangitis model.

6. α-GalCer-stimulated iNKT cells contributed to IFN-γ production by ASGM1$^+$ liver CD8$^+$ T cells in 2-OA-OVA immunized autoimmune cholangitis.

We sought to examine the pathogenic role of ASGM1$^+$ CD8 T cells in the 2-OA-OVA immunized autoimmune cholangitis model. Primary biliary cholangitis is considered a T_H1 disease with a significant increase in IFN-γ. Within the liver, there is a significantly higher frequency of IFN-γ mRNA-positive cells [41]. Previous studies have shown that IFN-γ can induce apoptosis of primary hepatocytes [42,43] and promote T_H1 immune responses [44], indicating that IFN-γ may play an important role in 2-OA-OVA immunized autoimmune cholangitis. First, we examined the IFN-γ deposition in the portal tract by immunohistochemical staining. Both α-ASGM1 and α-CXCR3 treatment in WT or KO mice decreased IFN-γ-positive area **(Fig. 6A)**. We also sorted out CD8 T cells from IHLs of PBC mice and observed that IFN-γ but not TNF-α and IL-4 expression was suppressed under α-ASGM1 treatment **(Fig. 6B)**. Thus, it was suggesting that ASGM1$^+$ liver T_{RM} cell population contributed to IFN-γ production in autoimmune cholangitis.

However, α-GalCer, utilized for exacerbation of cholangitis, could activate iNKT cells with hypersecretion of IFN-γ and IL-4 [39,45]. Thus, it is important to investigate the

doi:10.6342/NTU202202017

interaction of iNKT cells and the ASGM1$^+$ liver T_{RM} population. First, we determined the IFN-γ and IL-4 levels of α-GalCer-treated mice under anti-ASGM1 treatment, as α-GalCer induced the hypersecretion of IFN-γ and peaked at 18 hours post-α-GalCer induction. However, the IFN-γ production was decreased at both time points by α-ASGM1 pre-treatment **(Fig. 6C)**. However, the IL-4 production was not affected. IHLs were harvested 24 hours post-α-GalCer induction, and we found that the CD8$^+$ CD69$^+$ T cell population was decreased **(Fig. 6D)**. The results implied that activated iNKT cells continued to activate ASGM1$^+$ liver T_{RM} which contributed to IFN-γ production. To further analyze their interaction more specifically, we sorted out ASGM1$^+$/ ASGM1$^-$ CD8 T cells respectively then co-cultured with NKT cells under α-GalCer stimulation. We observed that IFN-γ expression by ASGM1$^+$ CD8 T cells was much higher than ASGM1$^-$ ones **(Fig 6E)**. Taken together, these results demonstrated that depletion with α-ASGM1 contributed to less IFN-γ accumulation under autoimmune cholangitis, indicating that ASGM1$^+$ CD8 T cells were crucial in the pathogenesis of autoimmune cholangitis.

doi:10.6342/NTU202202017

Chapter 4 Discussion

Our study showed that α-ASGM1 treatment suppressed the 2-OA-OVA immunized autoimmune cholangitis both in wild-type and NFIL3-KO mice, whereas NFIL3-KO mice without depletion treatment still developed autoimmune hepatitis. This finding suggests that the specific ASGM1$^+$ CD8 T cell population within the liver played a crucial role in the development of 2-OA-OVA immunized autoimmune cholangitis. Furthermore, we identified an ASGM1$^+$ CD8 T cell population with a liver-resident phenotype that showed higher activation potential. Moreover, this population could be depleted by both α-ASGM1 and α-CXCR3, highlighting features of the liver T_{RM} phenotype. In our data, we found that ASGM1$^+$ CD8 liver T_{RM} cells were activated in 2-OA-OVA immunized autoimmune cholangitis and were able to release IFN-γ under iNKT cell activation. Moreover, ASGM1$^+$ CD8 T cells and other IFN-γ-producing cells were decreased by α-ASGM1 treatment. In addition, we revealed that this distinct liver T_{RM} population was the main source of IFN-γ by CyTOF analysis. We, therefore, hypothesized that ASGM1$^+$ CD8 liver T_{RM} cells could be activated and prime other IHLs and lead to a T_H1-prone response. However, whether IFN-γ was responsible for mediating the interaction of ASGM1$^+$ CD8 T cells with other lymphocytes or not requires further investigation.

In this study, we used CyTOF analysis to investigate several cytotoxic molecules from ASGM1$^+$ CD8 T cells, and we found that ASGM1$^+$ CD8 T cells were not in charge

doi:10.6342/NTU202202017

of producing these molecules. Therefore, ASGM1$^+$ CD8 T cells were not thought to play a major role in 2 OA-OVA immunized autoimmune cholangitis by producing cytotoxic molecules. However, we found that IFN-γ was mainly produced by ASGM1$^+$ CD8 T cells in 2-OA-OVA immunized autoimmune cholangitis, and anti-ASGM1 treatment suppressed IFN-γ expression by depleting this population. We hypothesized that ASGM1$^+$ CD8$^+$ T cells mainly expressed IFN-γ to prime or interact with other effector cells and drive liver inflammation. Therefore, we used co-culture assays to study the interaction between ASGM1$^+$ CD8 T cells and other lymphocytes. ASGM1$^+$ CD8 T cells have been reported to be important for the induction of T_H1 response of producing IFN-γ from helper T cells [46]. In our experiments, ASGM1$^+$ CD8 T cells were sorted out from the liver and co-cultured with the α-GalCer-stimulated NKT cells isolated from the intrahepatic population. In **Fig. 6E**, the ASGM1$^+$ CD8 T cells exhibited higher IFN-γ production than ASGM1$^-$, suggesting that this population may be transactivated by other IHLs to produce IFN-γ. In the future, we will also harvest and co-culture biliary epithelial cells (BECs) to observe whether the apoptosis of BECs could be directly induced by activated ASGM1$^+$ CD8 T cells through IFN-γ production.

Liver CD8 T_{RM} cells expressed a high level of ASGM1, while NK cells were known to express ASGM1 and were especially abundant in the liver. However, we still wondered whether this distinct population persisted in the human liver or not and urgently needed

doi:10.6342/NTU202202017

further analyses. Liver CD8 T_{RM} cells have been reported to play a pathogenic role in the AIH, and glucocorticoid administration reduced liver inflammation by suppressing liver CD8 T_{RM} cell expansion [47]. This new study allowed us to explore therapeutic candidates that target liver-resident T cells. Furthermore, we can aim to disrupt the immune tolerance of the liver and fight tumors and infections as long as we adequately modulate $ASGM1^+$ CD8 T cells. Therefore, the contribution needs to be further investigated in practical or clinical applications.

As NK cells make up a large proportion of the $ASGM1^+$ population in the liver, the previous study reported that the cytotoxic activity, perforin expression, and CD128a (IL-8R, CXCR1) expression in NK cells were significantly increased in PBC patients. However, the cytokine produced by isolated NK cells was significantly reduced in PBC compared with controls [48]. In addition to NK cells, our data indicated that a specific population of $ASGM1^+$ CD8 liver T_{RM} cells played a critical factor in 2-OA-OVA immunized autoimmune cholangitis and could be depleted by anti-ASGM1 antisera. In our study, we pre-treated anti-ASGM1 before 2-OA-OVA priming, followed by continuous treatment twice weekly until sacrifice. To simulate the therapeutic application of human PBC patients, further experiments should be performed after the onset of PBC to observe whether the progressed disease could be reversed by anti-ASGM1 treatment. Therefore, the timing of depletion antibody treatment should be further investigated for

doi:10.6342/NTU202202017

better protection.

It has been reported that T_{RM}-derived IFN-γ is required for recruitment and communication. However, this mechanism has not been discussed further. It remained unclear whether IFN-γ signaling promotes tissue invasion by acting directly on the lymphocytes themselves. It could also occur indirectly by altering the gradient and triggering immune cell migration by releasing chemokines CXCL9 and CXCL10. In this work, we only knew that $ASGM1^+$ liver T_{RM} cells were the main IFN-γ-producing cells, and the accumulation of IFN-γ was positively correlated with the infiltration. However, we should utilize specific conditional KO mice to investigate the role of IFN-γ in communicating $ASGM1^+$ CD8 T cells and other immune cells. At the very least, IFN-γ-deficient mice should be urgently evaluated. Other effector cytokines or factors should also be studied in detail in the future.

In our previous study, viral clearance was suppressed by anti-ASGM1 treatment in the HBV hydrodynamic transfection model. Furthermore, the spotting units in the HBsAg IFN-γ ELISpot assay were also reduced by the treatment. In this study, mice were immunized with 2-OA-OVA and monitored for $ASGM1^+$ CD8 liver T_{RM} cell responses. However, the details of the TCR repertoire have not yet been characterized. Previous studies have reported that transgenic mice such as PbT-I and OT-I strains also constitute naïve TCR repertoire. Furthermore, T cell activation and IL-15 were reported to be

doi:10.6342/NTU202202017

important for the formation of liver T_{RM} cells [49]. Despite using OVA-conjugated 2-OA, it was still questionable whether the activation of $ASGM1^+$ liver T_{RM} cells depends on the endogenous TCR rearrangement and drives the inflammation. Therefore, further analysis by TCR sequencing is needed to identify their differences and how they evolved into the specific cell lineage.

Mouse CD8 hepatic T_{RM} cells were found to express ASGM1. In addition, NK cells as another population expressing ASGM1, which was especially abundant in the liver. Sung et al., 2021 demonstrated that the adoptively transferred $ASGM1^+$ CD8 T cells were competent to engraft and persist in the liver. However, whether ASGM1 could function as a marker for liver residency requires further investigation. Although our preliminary study showed that the recovery of depleted $ASGM1^+$ CD8 T cells was reduced after blocking asialoglycoprotein receptor 1 (ASGPR1), suggesting that ASGPR1 may be a receptor for ASGM1. Thus, ASGM1-bound protein deserves in-depth investigation by immunoprecipitation or knockout genes for further clinical applications. Also, the global genetic profile of the $ASGM1^+$ CD8 T cells also remained unclear, as these cells may be a mixed population. In addition to the comparison of $ASGM1^+$ CD8 T cells with previously reported T_{RM} cells by transcriptomic analysis in our previous study [17], we still need to perform detailed single-cell RNA sequencing to further identify specificities and reveal specific intrahepatic populations. Furthermore, we still need to investigate the

doi:10.6342/NTU202202017

ASGM1 expression in human intrahepatic lymphocytes. If ASGM1 alone is sufficient for liver residency, there will be more therapies applicable.

doi:10.6342/NTU202202017

Chapter 5 Figures

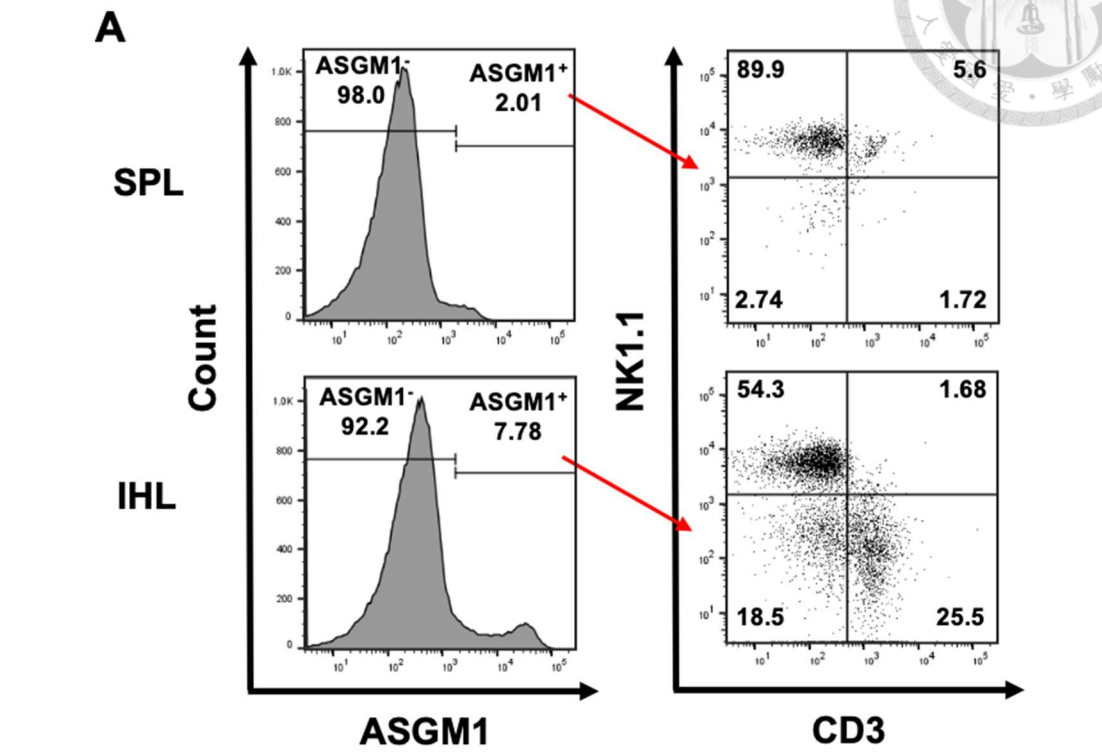

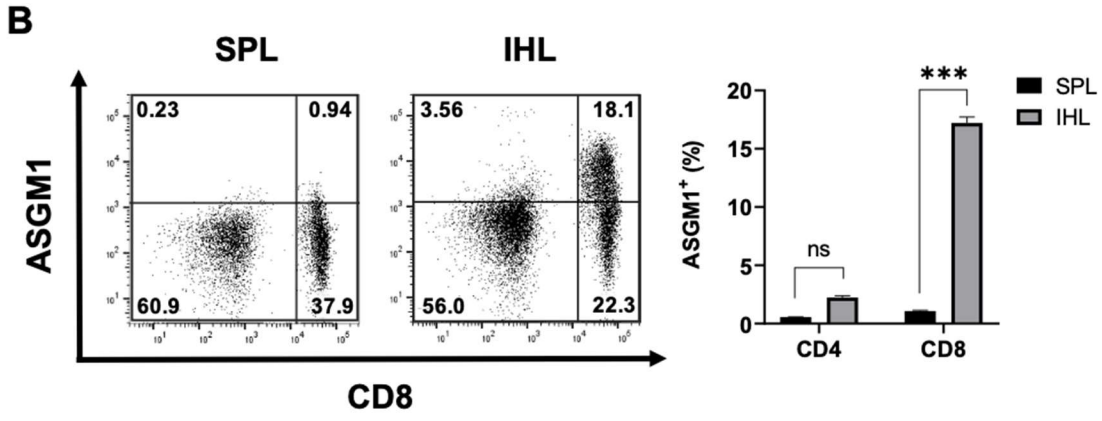

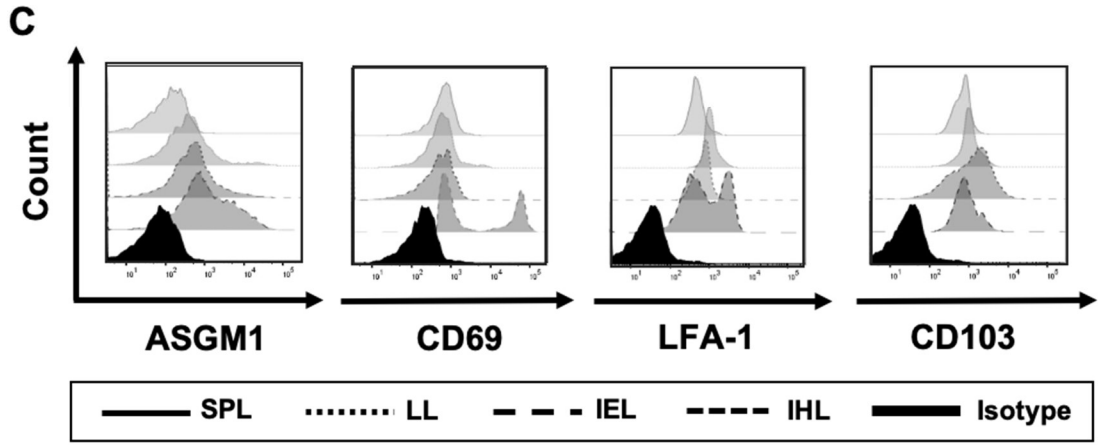

doi:10.6342/NTU202202017

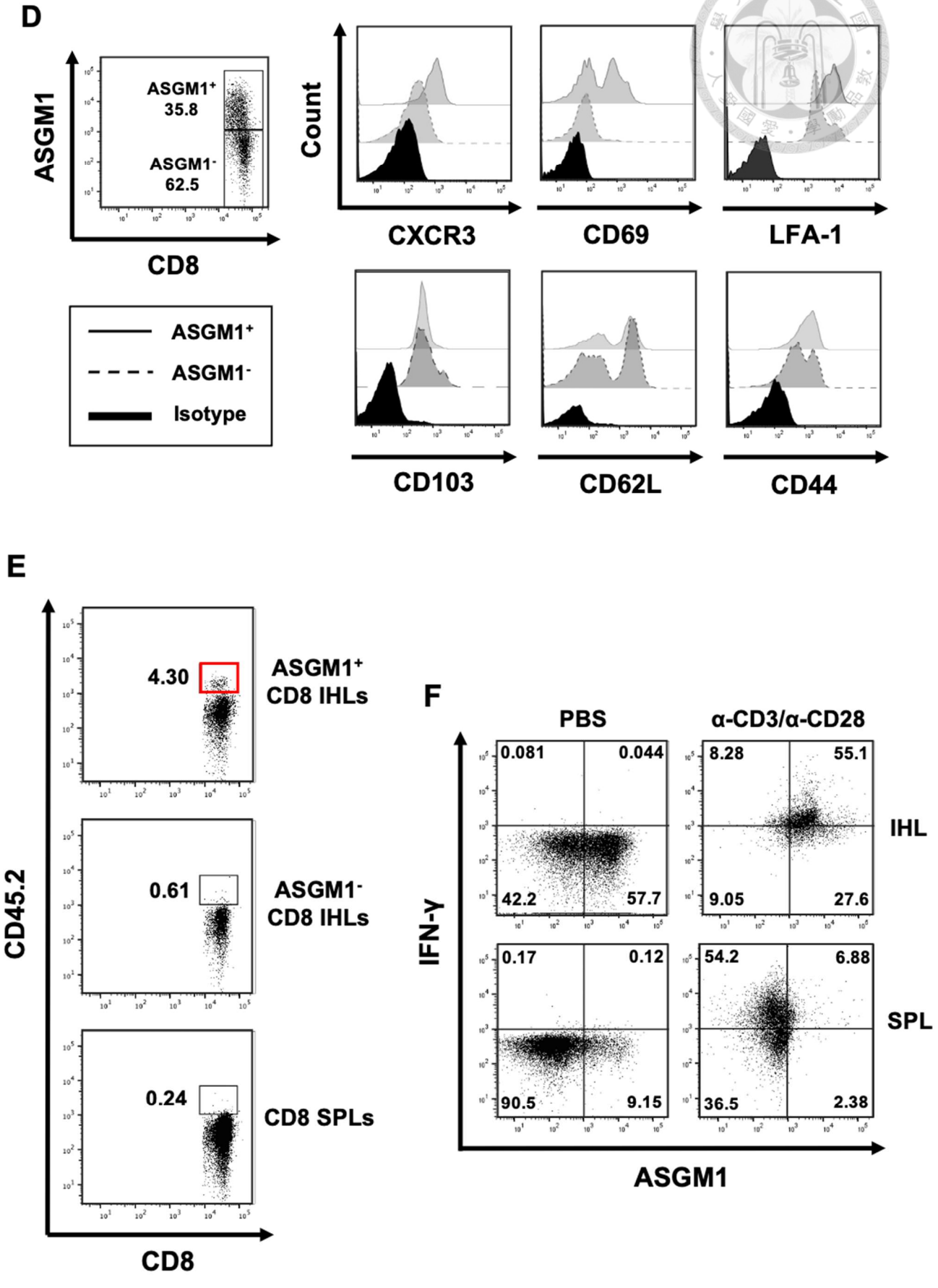

doi:10.6342/NTU202202017

Figure 1. A distinct ASGM1$^+$ CD8$^+$ T cell population persisted in the liver and exhibited phenotypic and functional liver T_{RM} characteristics. (A) The total ASGM1$^+$ population was acquired for determining NK cell and CD3$^+$ T cell composition. (B) The ASGM1$^+$ population of CD4$^+$/ CD8$^+$ T cells in SPLs and IHLs was analyzed. Data was shown in pre-gated NK1.1$^-$ CD3$^+$ cells. (C) Splenocytes (SPLs), lung lymphocytes (LLs), intraepithelial cells of the intestines (IELs), and intrahepatic lymphocytes (IHLs) were harvested within individual mouse, respectively. Tissue residency-related surface markers of CD8$^+$ T cells were analyzed. Data was shown in pre-gated NK1.1$^-$ CD3$^+$ CD8$^+$ cells. (D) Detailed T_{RM} surface markers of ASGM1$^+$ CD8 T cells were compared with ASGM1$^-$ counterparts. Data was shown in pre-gated NK1.1$^-$ CD3$^+$ CD8$^+$ cells. (E) Donor (CD45.2$^+$) IHLs were sorted into ASGM1$^+$ and ASGM1$^-$ CD8 T cells and adoptively transferred into recipients (CD45.1$^+$) mice. After 48 hours, IHLs from the recipient mice were analyzed. (F) IHLs and SPLs were harvested and isolated into CD3$^+$ T cells. For *ex vivo* activation, cells were cultured with α-CD3/α-CD28 for 48 hours, and the analysis of the IFN-γ-producing population was determined by intracellular staining. Data represented at least three independent experiments with each group comprising three mice or more. Statistics were shown as the mean ± SEM. *$p < 0.05$, **$p < 0.01$, ***$p < 0.001$ between selected relevant comparisons by Student's t-test.

doi:10.6342/NTU202202017

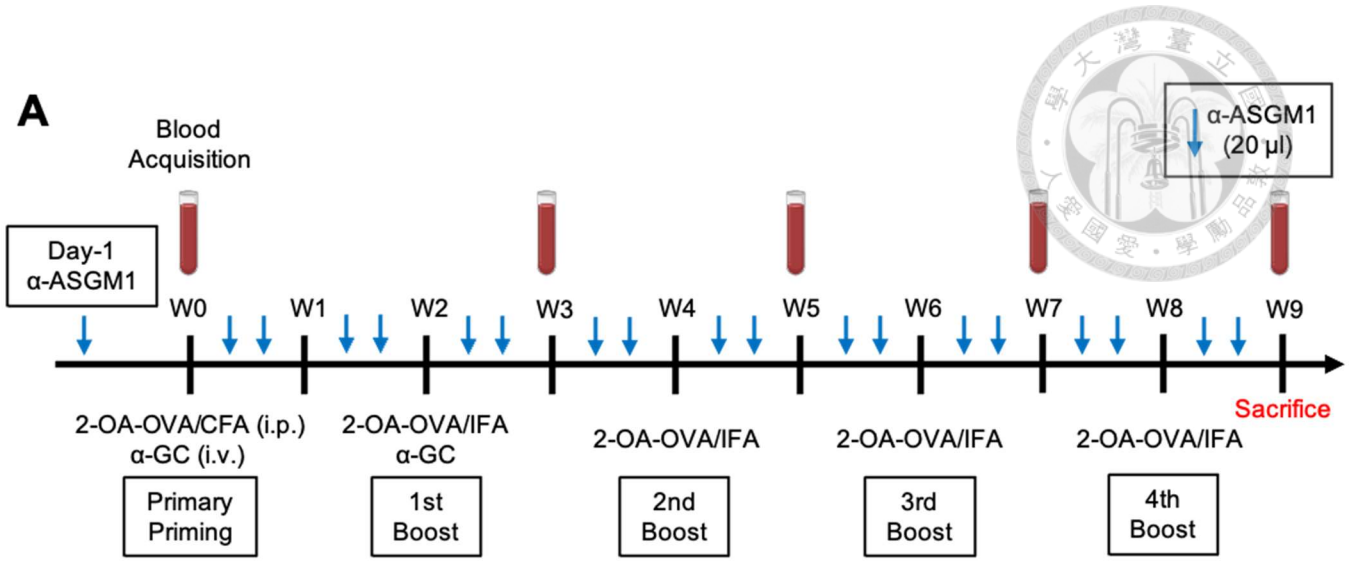

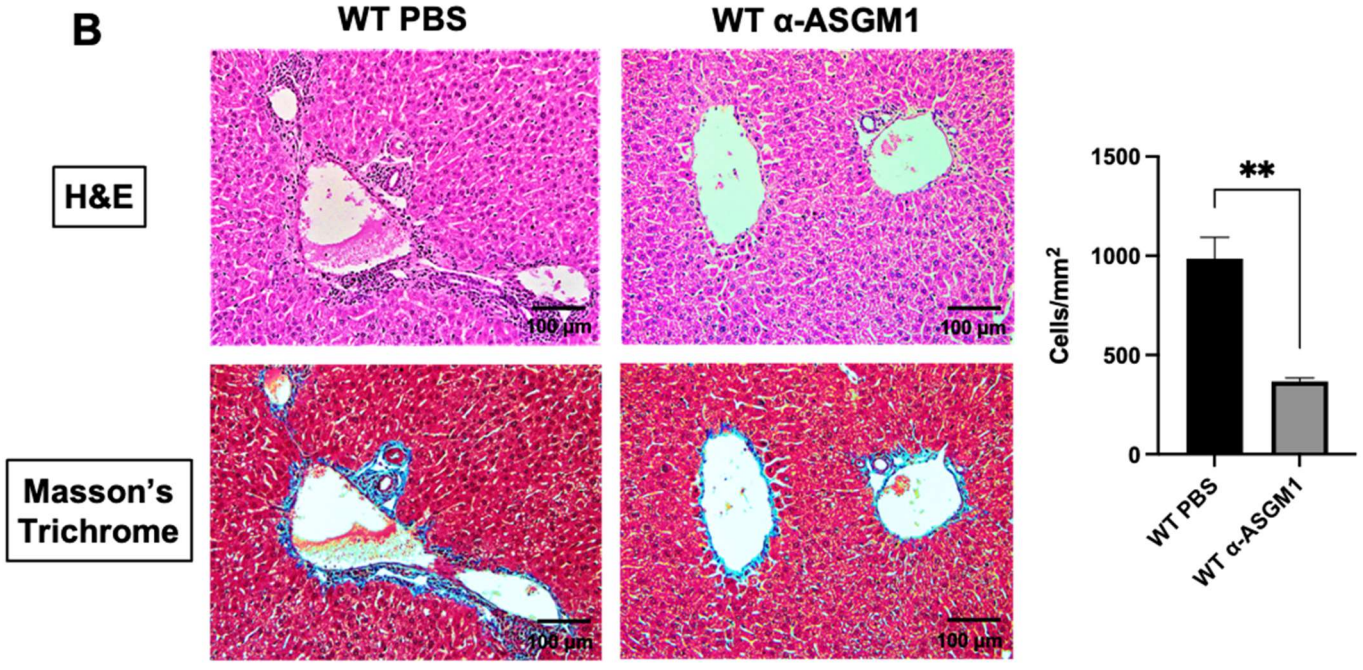

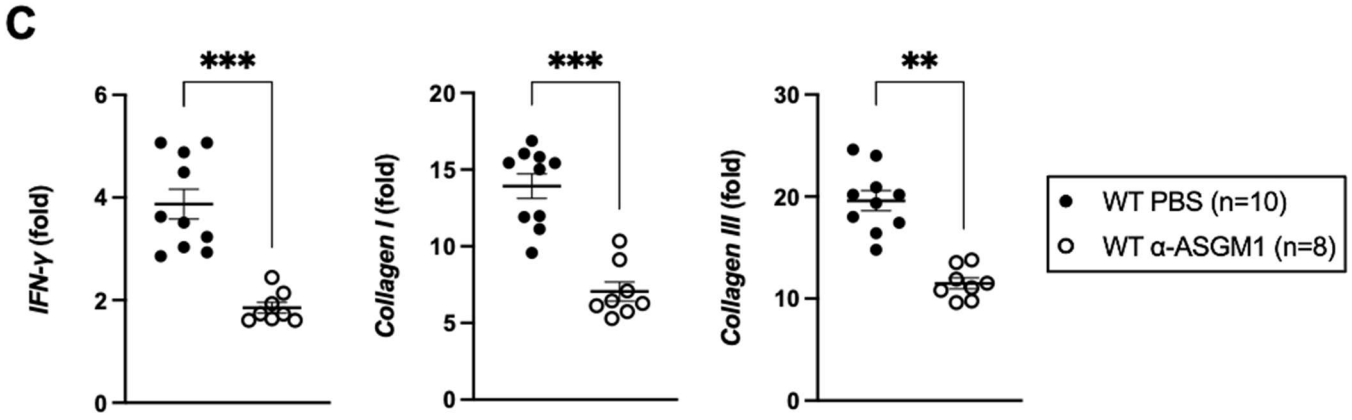

doi:10.6342/NTU202202017

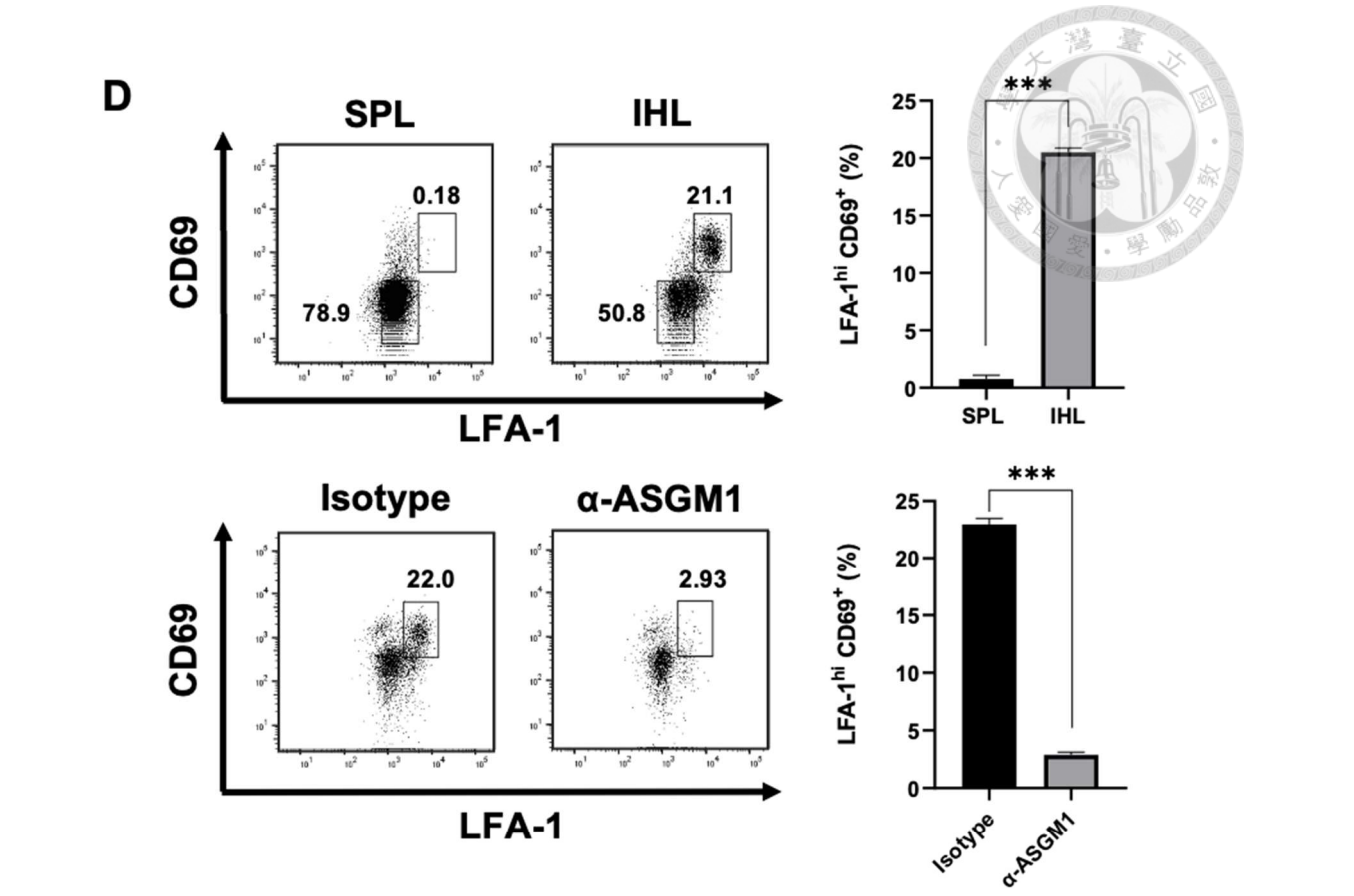

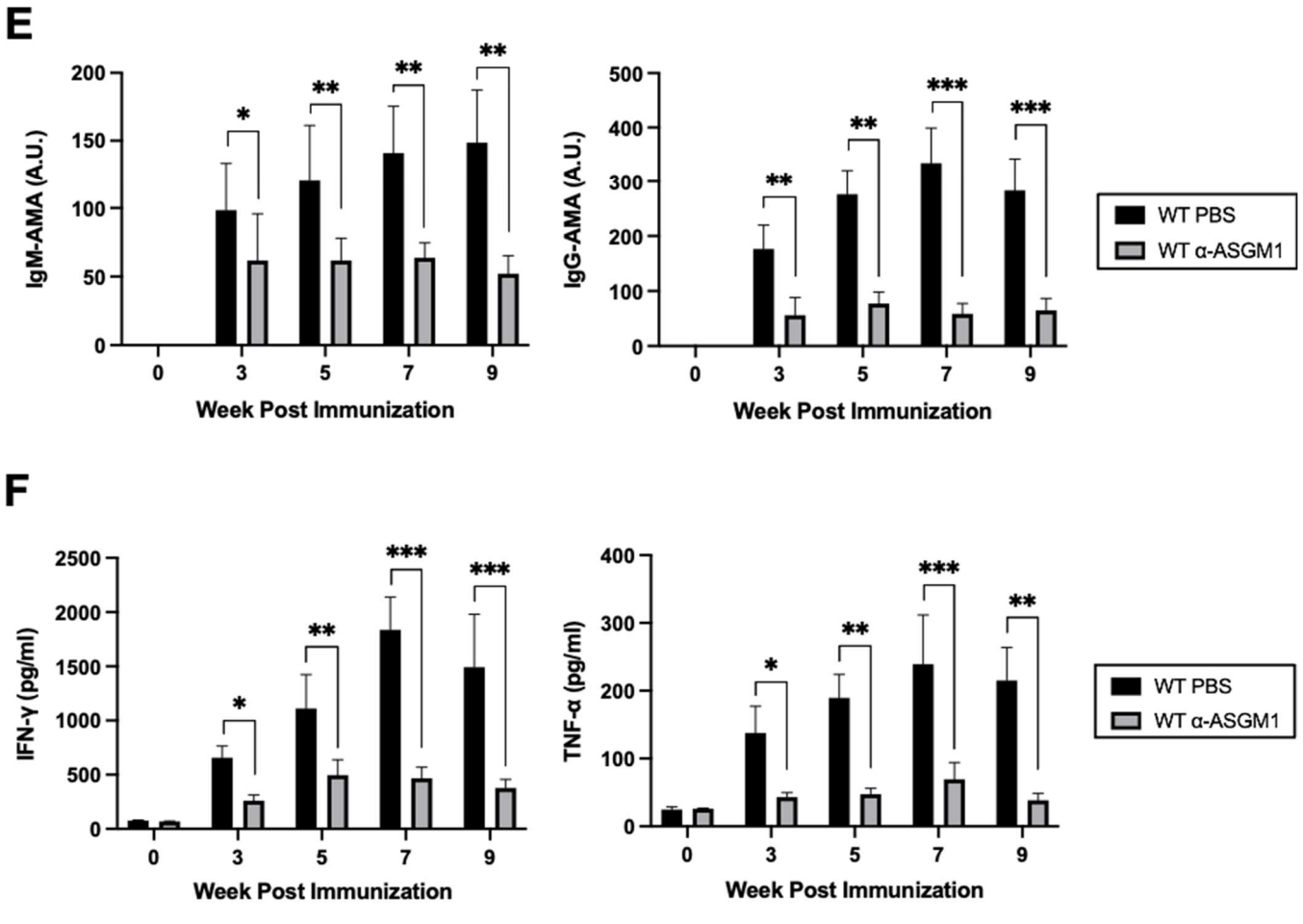

doi:10.6342/NTU202202017

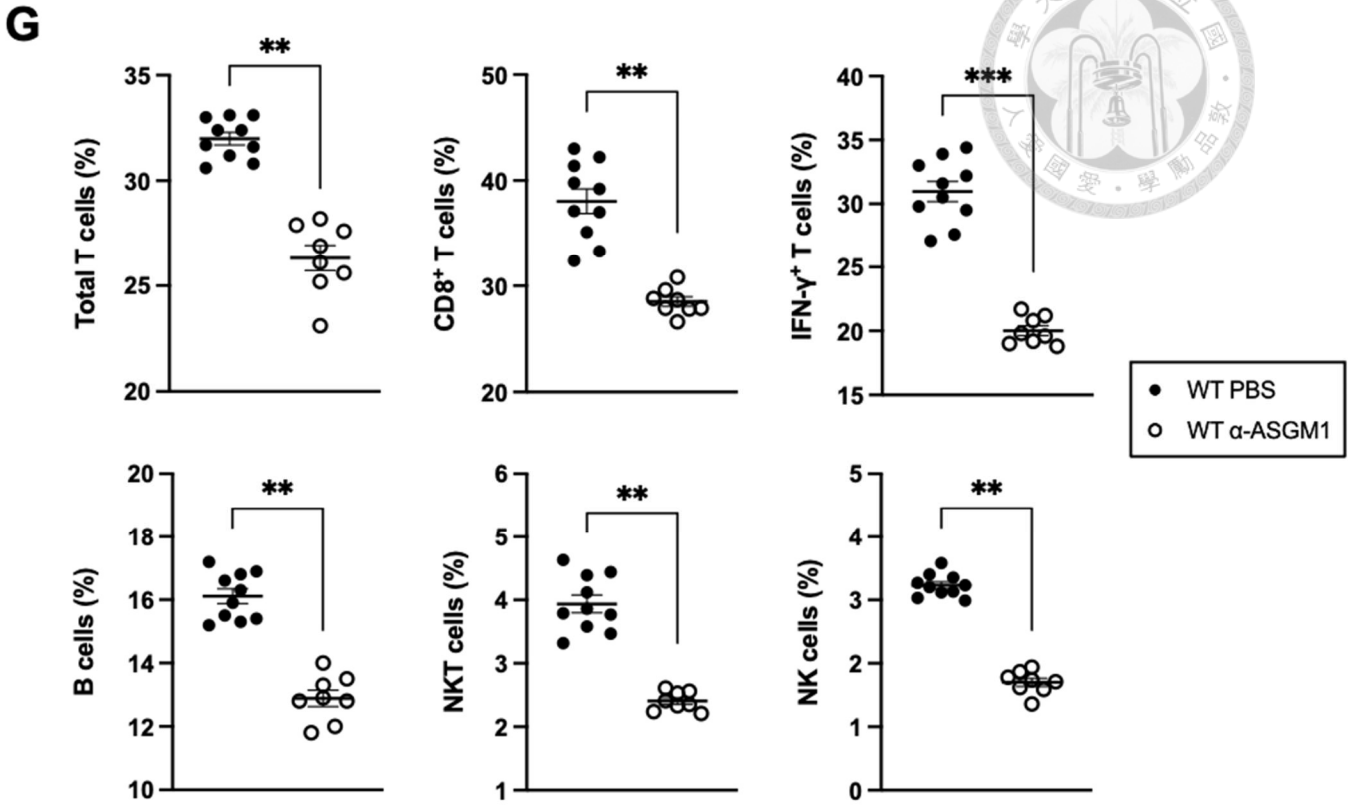

doi:10.6342/NTU202202017

Figure 2. Autoimmune cholangitis and liver fibrosis were suppressed by α-ASGM1 treatment in 2-OA-OVA immunized autoimmune cholangitis. (A) Experimental time course of 2-OA-OVA immunized autoimmune cholangitis model establishment utilizing C57BL/6 (WT) mice, and IHL was depleted through α-ASGM1 treatment intraperitoneally (i.p.) *in vivo*. (B) Representative H&E staining and Masson's Trichrome staining (× 200 magnification) of liver sections. The collagen fibers were stained blue. (C) The expression levels of IFN-γ, collagen I, and, collagen III mRNA in the liver were determined by RT-qPCR. Fold changes were normalized to naïve control. (D) The presence of the LFA-1^{hi} $CD69^{+}$ population in SPL and IHL was analyzed. For depletion, α-ASGM1 was pre-treated intraperitoneally 24 hours before sacrifice, and IHL were harvested. Cells were pre-gated from $NK1.1^{-}$ $CD3^{+}$ $CD8^{+}$. (E) Serum levels of anti-PDC-E2 IgM and IgG were determined by ELISA. A.U., arbitrary unit. (F) Serum levels of IFN-γ and TNF-α were determined by ELISA. (G) The percentage of total T, $CD8^{+}$ T, IFN-γ^{+} T, B, NK, and NKT cell populations in the liver were quantified by flow cytometry. Each dot represents an individual mouse. *$p < 0.05$; **$p < 0.01$; ***$p < 0.001$ between selected relevant comparisons by Student's t-test or one-way ANOVA followed by Tukey multiple comparison test.

doi:10.6342/NTU202202017

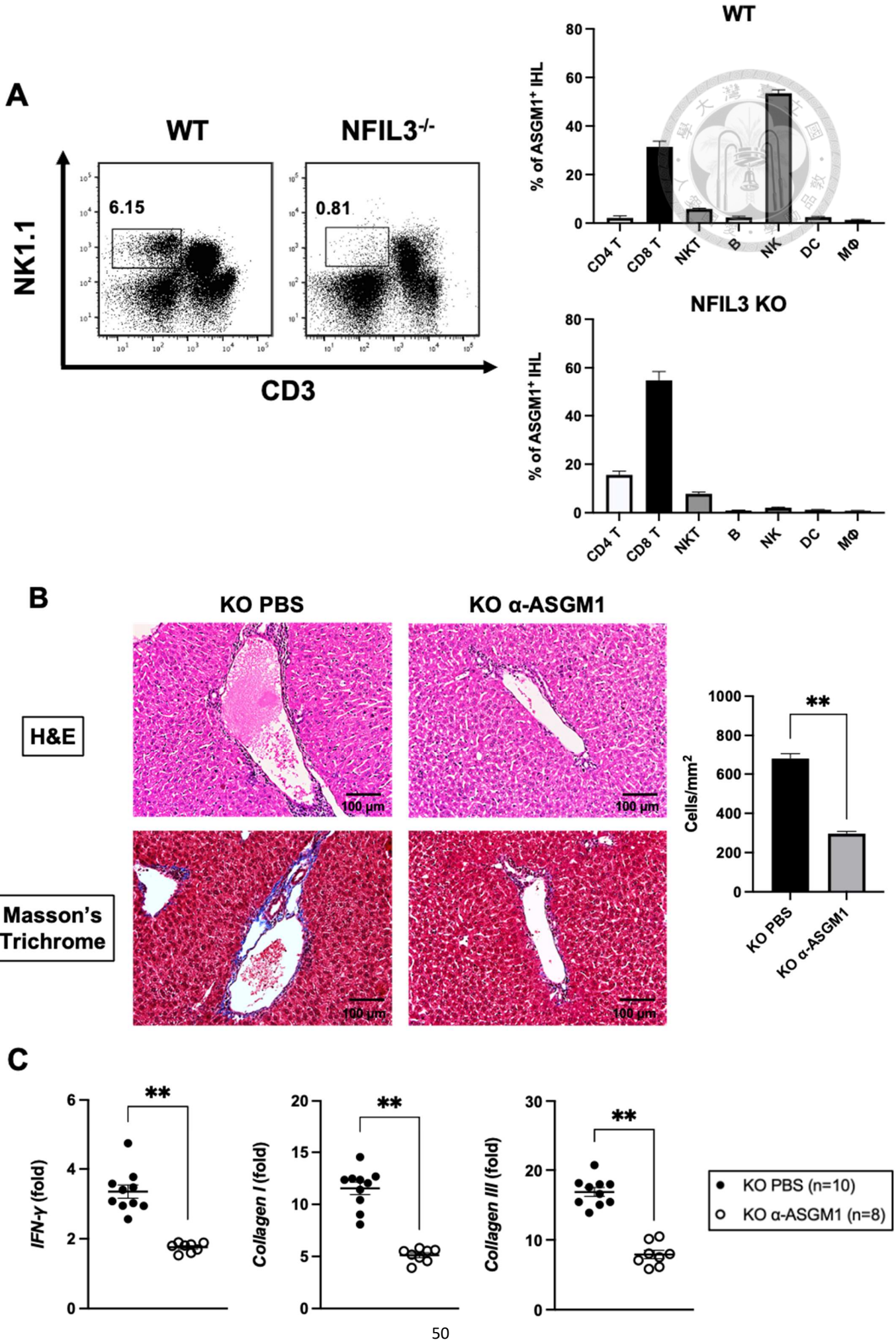

doi:10.6342/NTU202202017

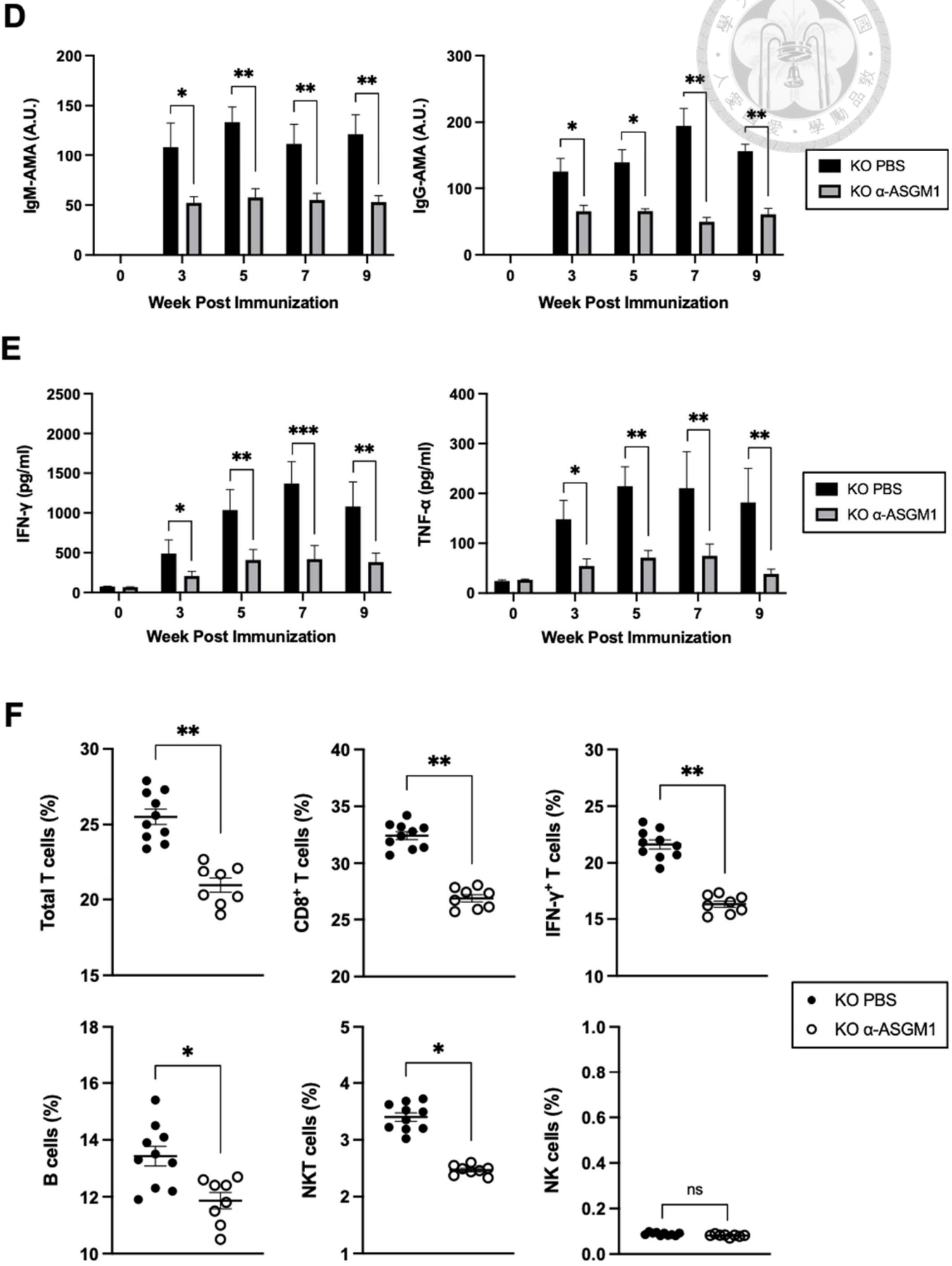

doi:10.6342/NTU202202017

Figure 3. 2-OA-OVA immunized autoimmune cholangitis was suppressed by α-ASGM1 treatment through an NK cell-independent mechanism. (A) NK cells were observed in IHL harvested from WT and KO mice. Cells were pre-gated from $NK1.1^+$ $CD3^-$. $ASGM1^+$ cells were sorted from IHLs, and quantification of the percentage of the indicated cells in IHLs from WT and $NFIL3^{-/-}$ mice was shown. (B) Representative H&E staining and Masson's Trichrome staining (× 200 magnification) of liver sections. The collagen fibers were stained blue. (C) The expression levels of IFN-γ, collagen I, and collagen III mRNA in the liver were determined by RT-qPCR. Fold changes were normalized to naïve control. (D) Serum levels of anti-PDC-E2 IgM and IgG were determined by ELISA. A.U., arbitrary unit. (E) Serum levels of IFN-γ and TNF-α were determined by ELISA. (F) The percentage of total T, $CD8^+$ T, IFN-γ^+ T, B, NK, and NKT cell populations in the liver were quantified by flow cytometry. Each dot represents an individual mouse. *$p < 0.05$; **$p < 0.01$; ***$p < 0.001$ between selected relevant comparisons by Student's t-test or one-way ANOVA followed by Tukey multiple comparison test.

doi:10.6342/NTU202202017

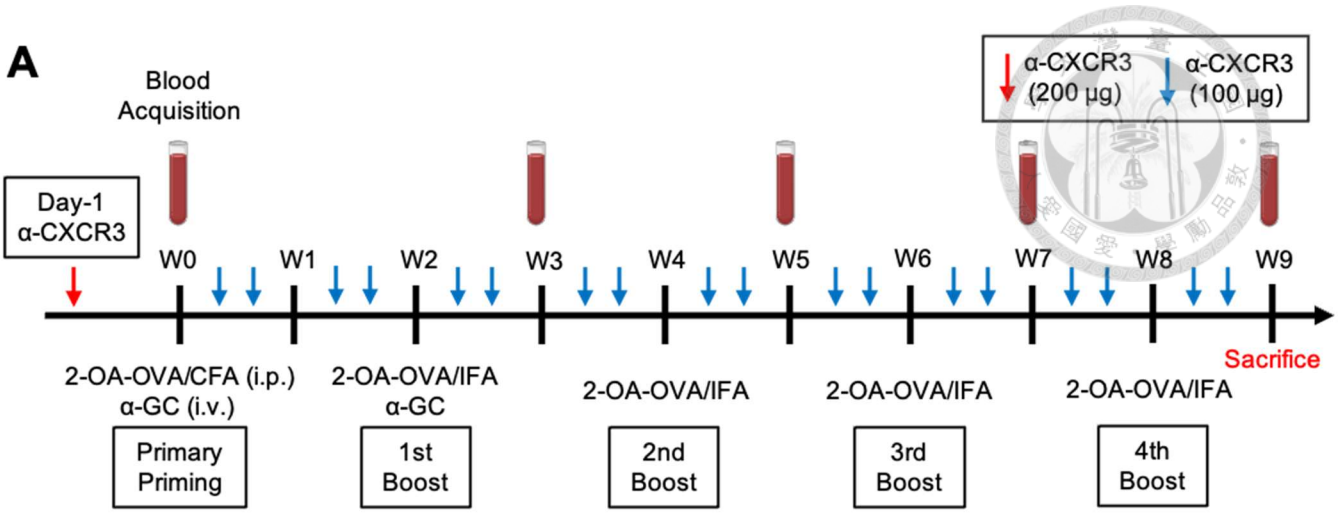

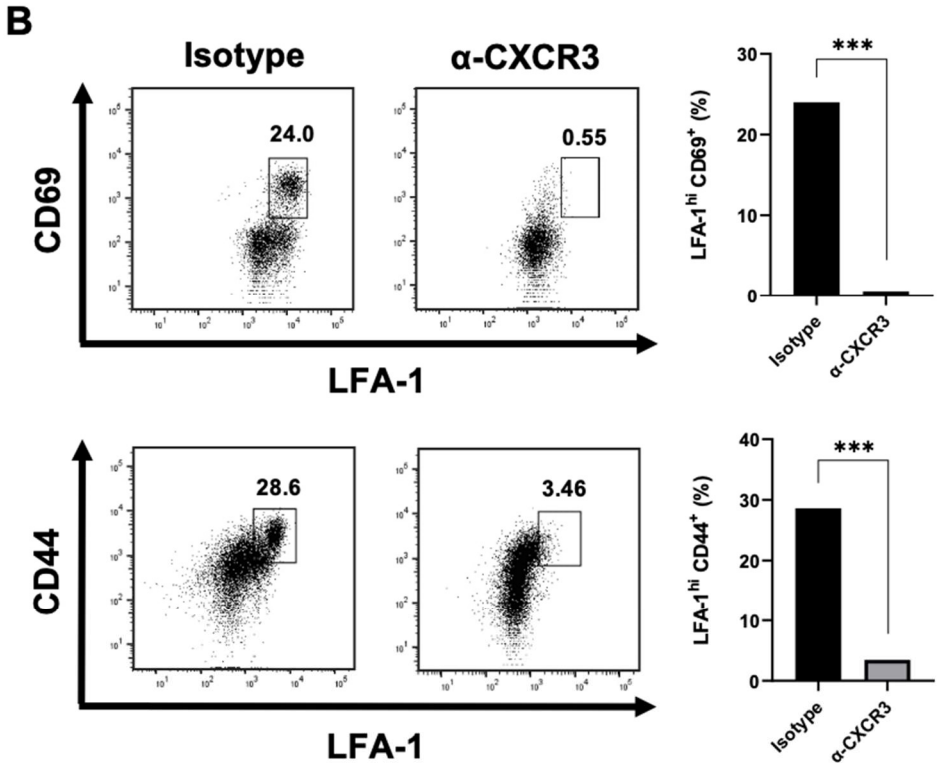

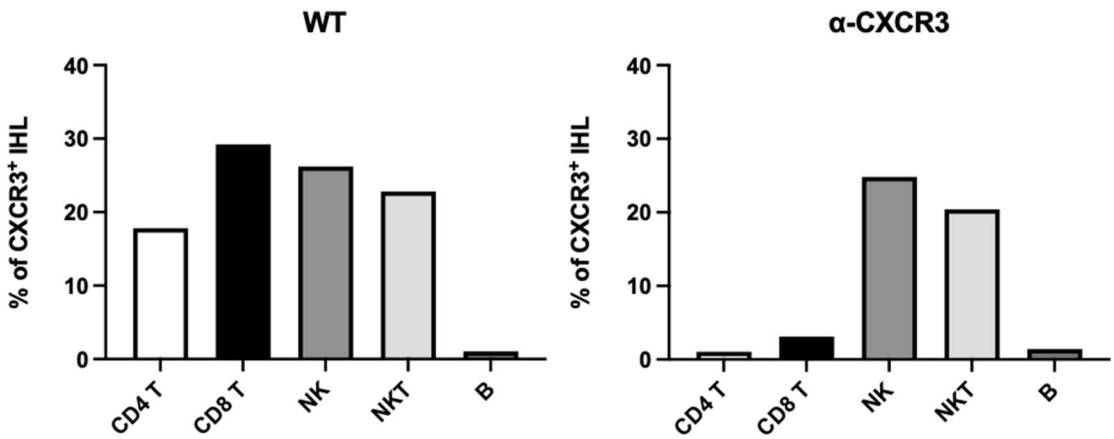

doi:10.6342/NTU202202017

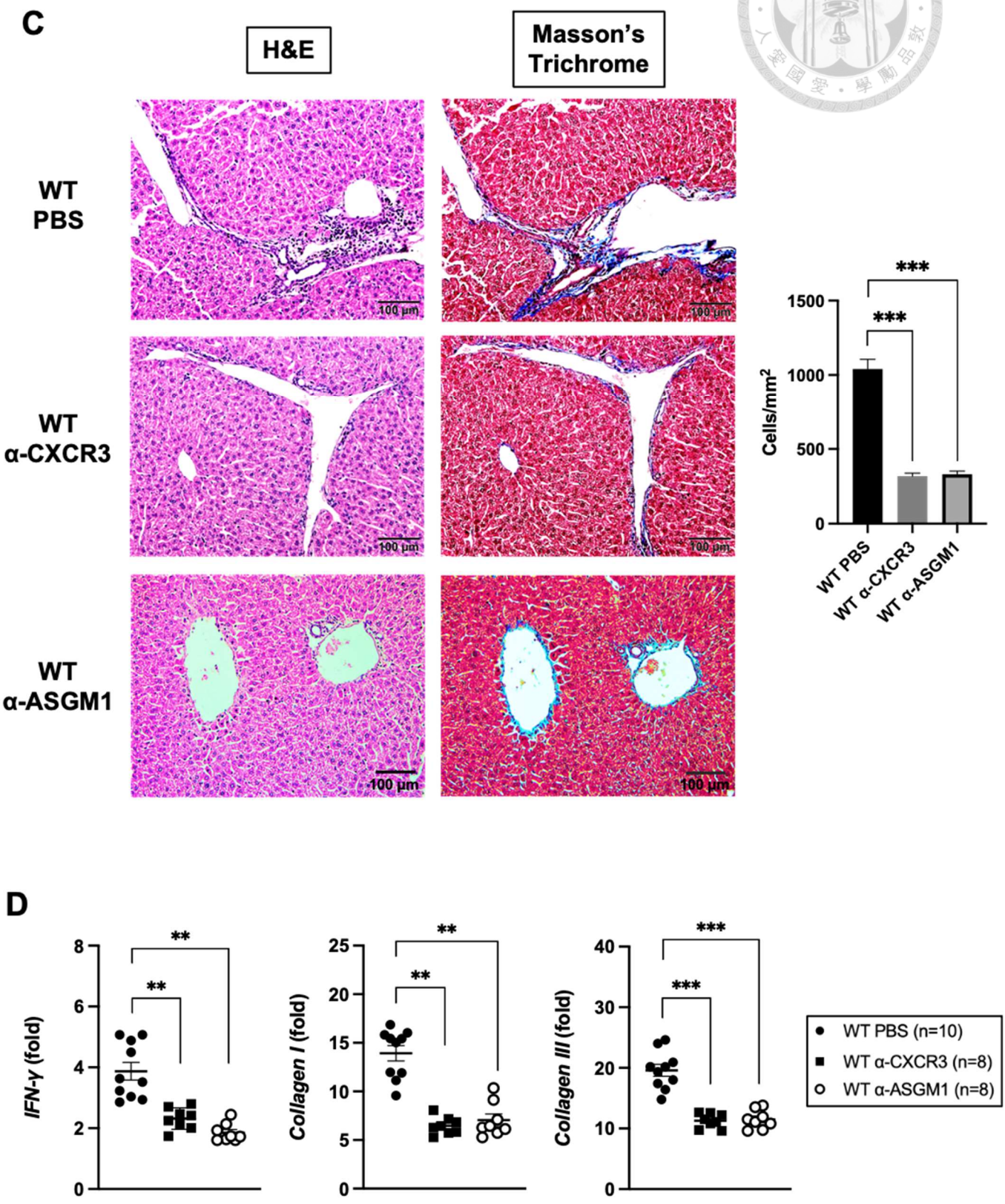

doi:10.6342/NTU202202017

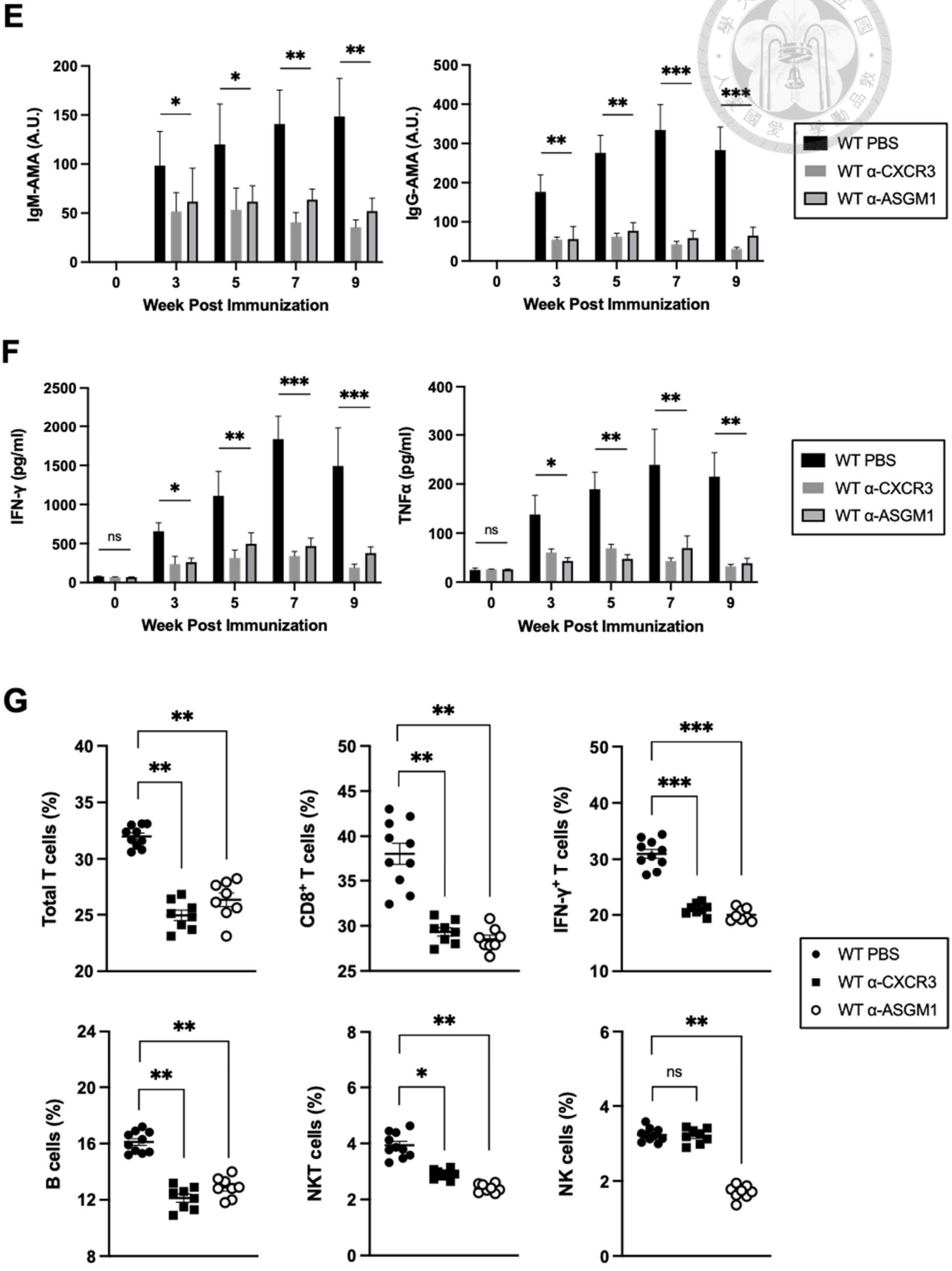

doi:10.6342/NTU202202017

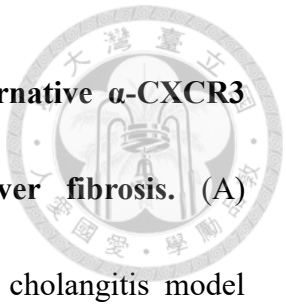

Figure 4. Depleting ASGM1$^+$ liver CD8$^+$ T cells through alternative α-CXCR3 treatment also suppressed autoimmune cholangitis and liver fibrosis. (A) Experimental time course of 2-OA-OVA immunized autoimmune cholangitis model establishment, and IHL was depleted through α-CXCR3 treatment intravenously (i.v.) *in vivo*. (B) LFA-1^{hi} CD69$^+$ and LFA-1^{hi} CD44$^+$ population was analyzed. α-CXCR3 was pre-treated intravenously 72 hours (200 μg) and 24 hours (100 μg) before sacrifice, and IHL was harvested. Cells were pre-gated from NK1.1$^-$ CD3$^+$ CD8$^+$. CXCR3$^+$ cells were sorted from IHLs, and the percentage of the indicated cells in IHLs from WT and α-CXCR3-treated mice was quantified. (C) Representative H&E staining and Masson's Trichrome staining (× 200 magnification) of liver sections. The collagen fibers were stained blue. (D) The expression levels of IFN-γ, collagen I, and collagen III mRNA in the liver were determined by RT-qPCR. Fold changes were normalized to naïve control. (E) Serum levels of anti-PDC-E2 IgM and IgG were determined by ELISA. A.U., arbitrary unit. (F) Serum levels of IFN-γ and TNF-α were determined by ELISA. (G) The percentage of total T, CD8$^+$ T, IFN-γ$^+$ T, B, NK, and NKT cell populations in the liver were quantified by flow cytometry. Each dot represents an individual mouse. *$p < 0.05$; **$p < 0.01$; ***$p < 0.001$ between selected relevant comparisons by Student's t-test or one-way ANOVA followed by Tukey multiple comparison test.

doi:10.6342/NTU202202017

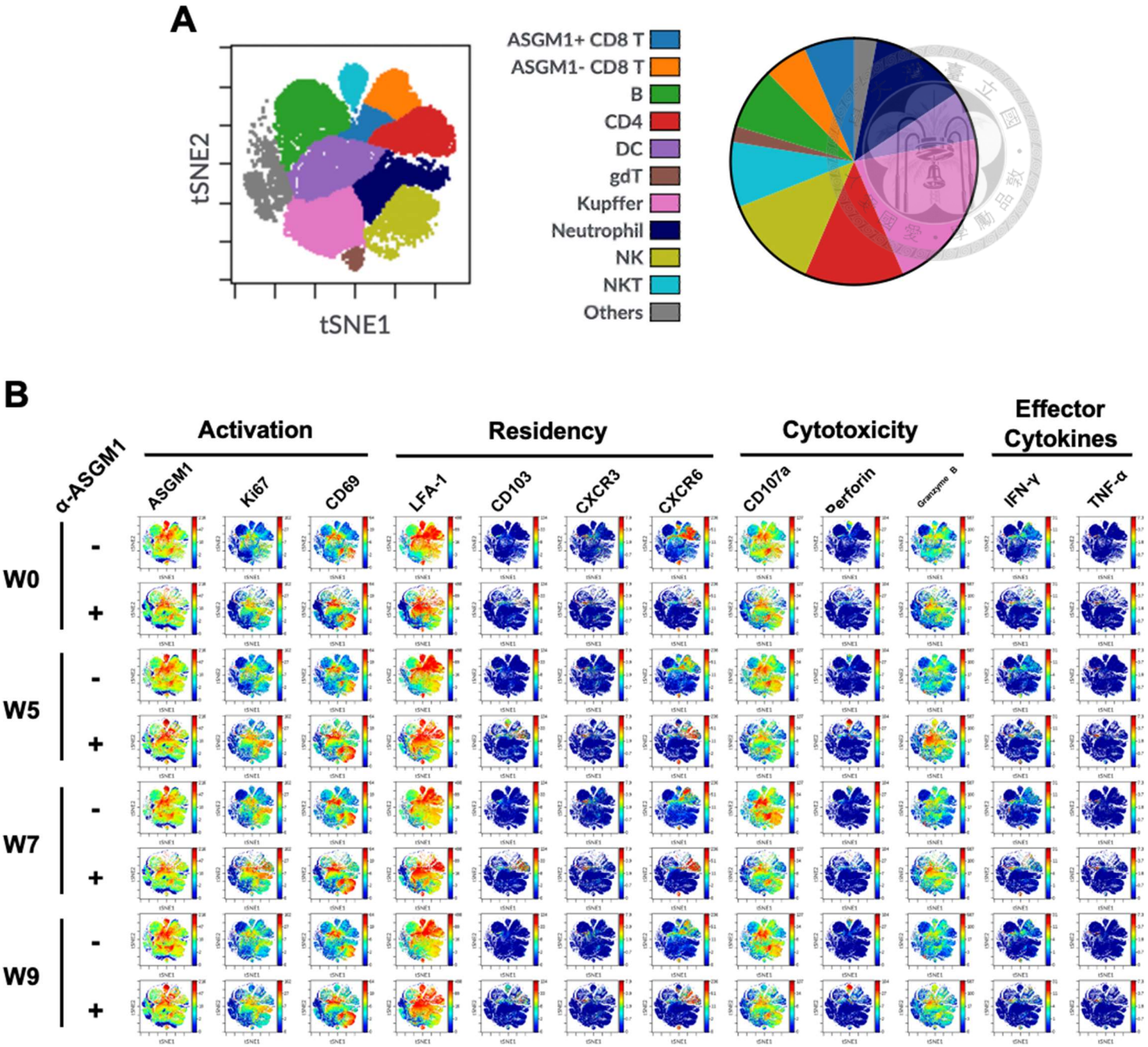

doi:10.6342/NTU202202017

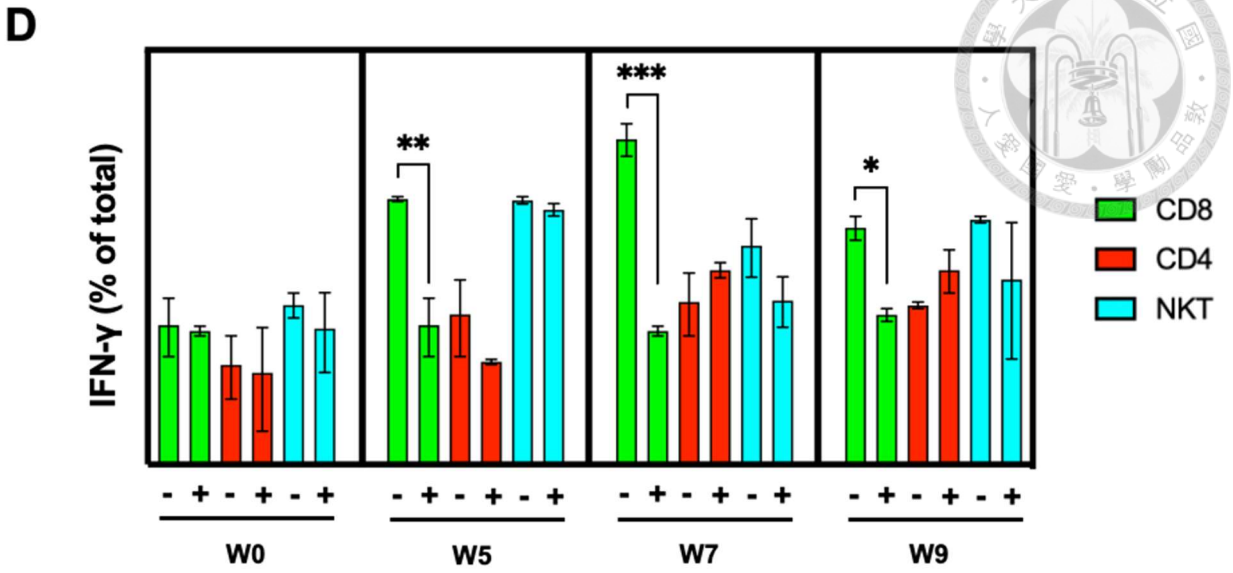

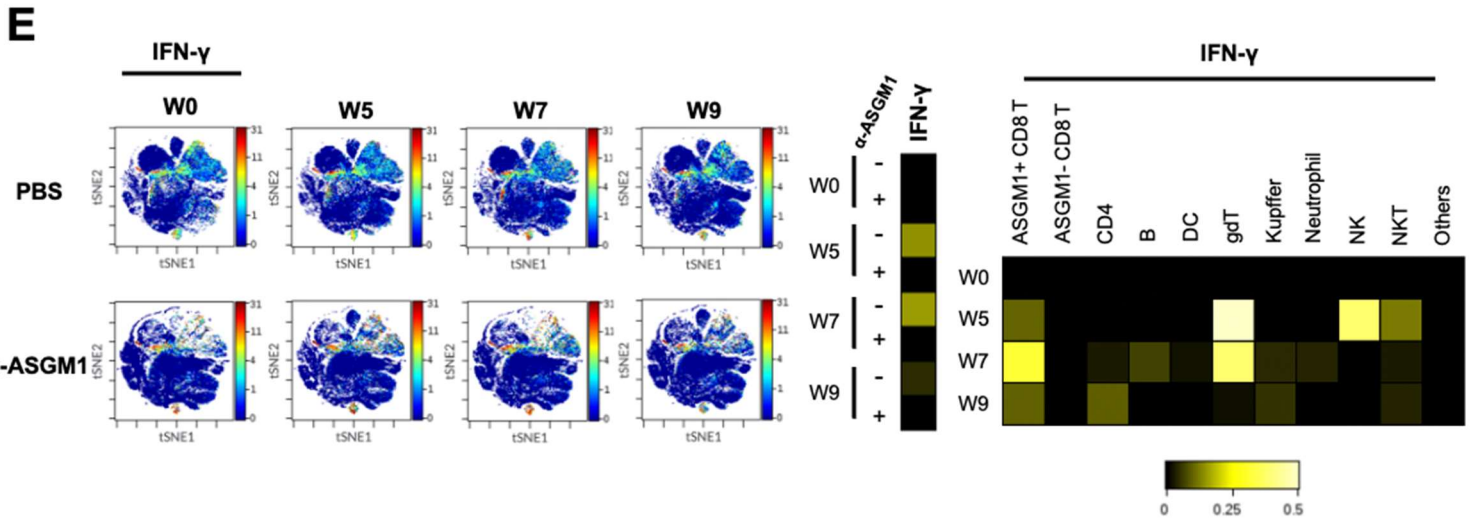

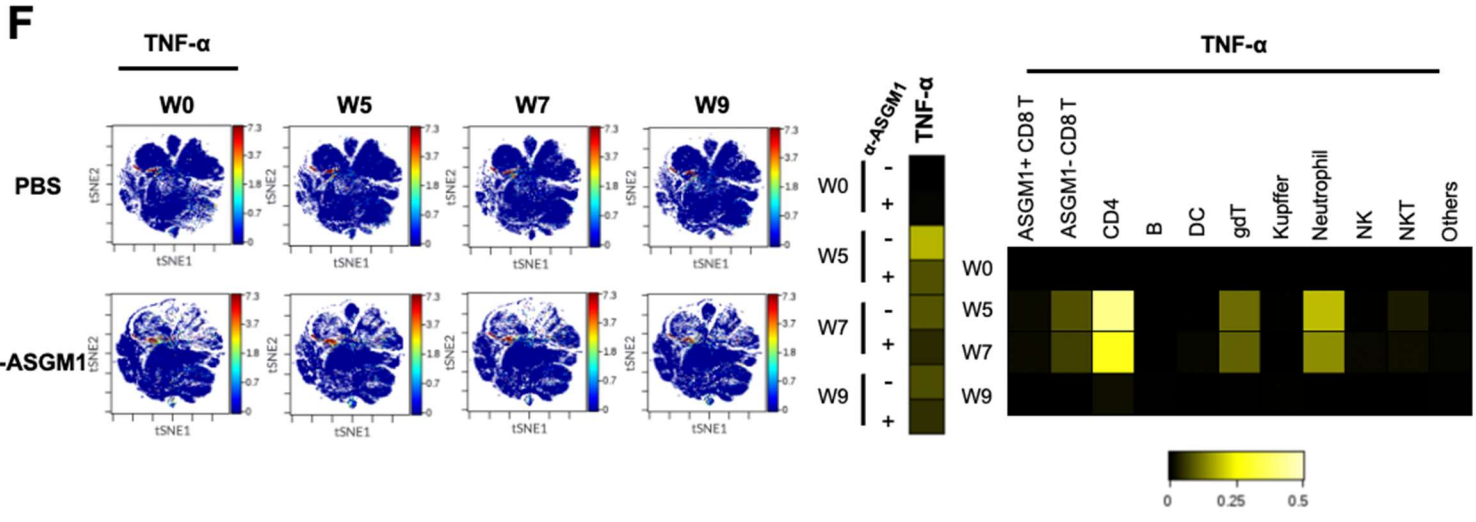

doi:10.6342/NTU202202017

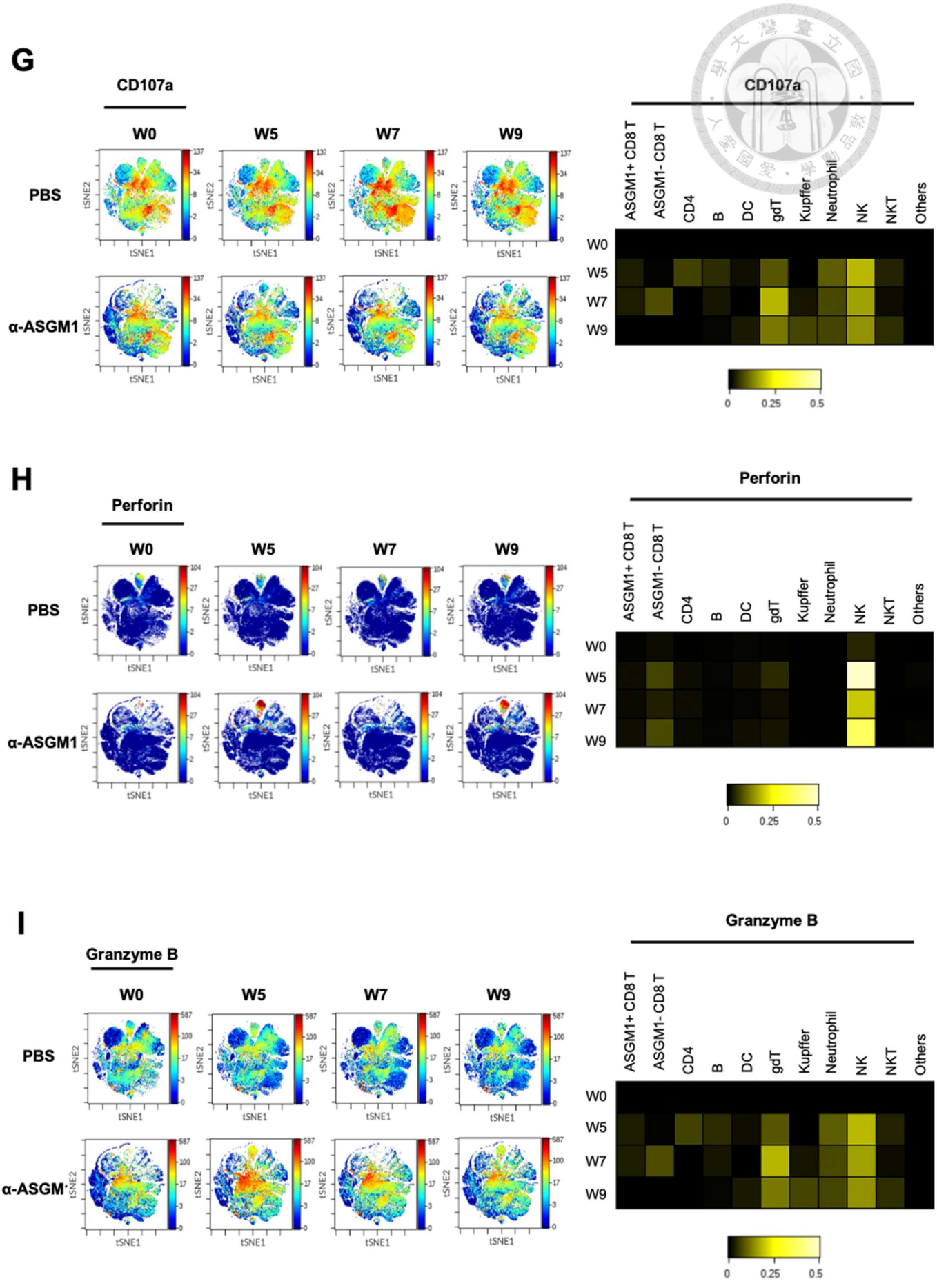

doi:10.6342/NTU202202017

Figure 5. IFN-γ was produced by activated ASGM1$^+$ liver CD8$^+$ T cells under 2-OA-OVA immunized autoimmune cholangitis. (A)-(I) Mice were intravenously injected with Golgi-block 1 hour before sacrifice. A panel of 34 surface markers and 5 intracellular markers was used to characterize intrahepatic leukocytes by CyTOF. IHLs were collected from different time point after 2-OA-OVA immunization. (A) IHLs were separated into different subsets by specific surface markers, respectively. (B) Markers representative for different functions were compared with/ without α-ASGM1 treatment. (C) The proportion of different cell subsets in different time intervals of PBC mice with/ without α-ASGM1 treatment were analyzed and presented by stacked bar plot. (D) Dynamic change IFN-γ expression of specific populations was investigated. (E)-(I) Kinetics of IFN-γ, TNF-α, CD107, perforin, and granzyme B expression level and producing populations were analyzed. *$p < 0.05$; **$p < 0.01$; ***$p < 0.001$ between selected relevant comparisons by Student's t-test.

doi:10.6342/NTU202202017

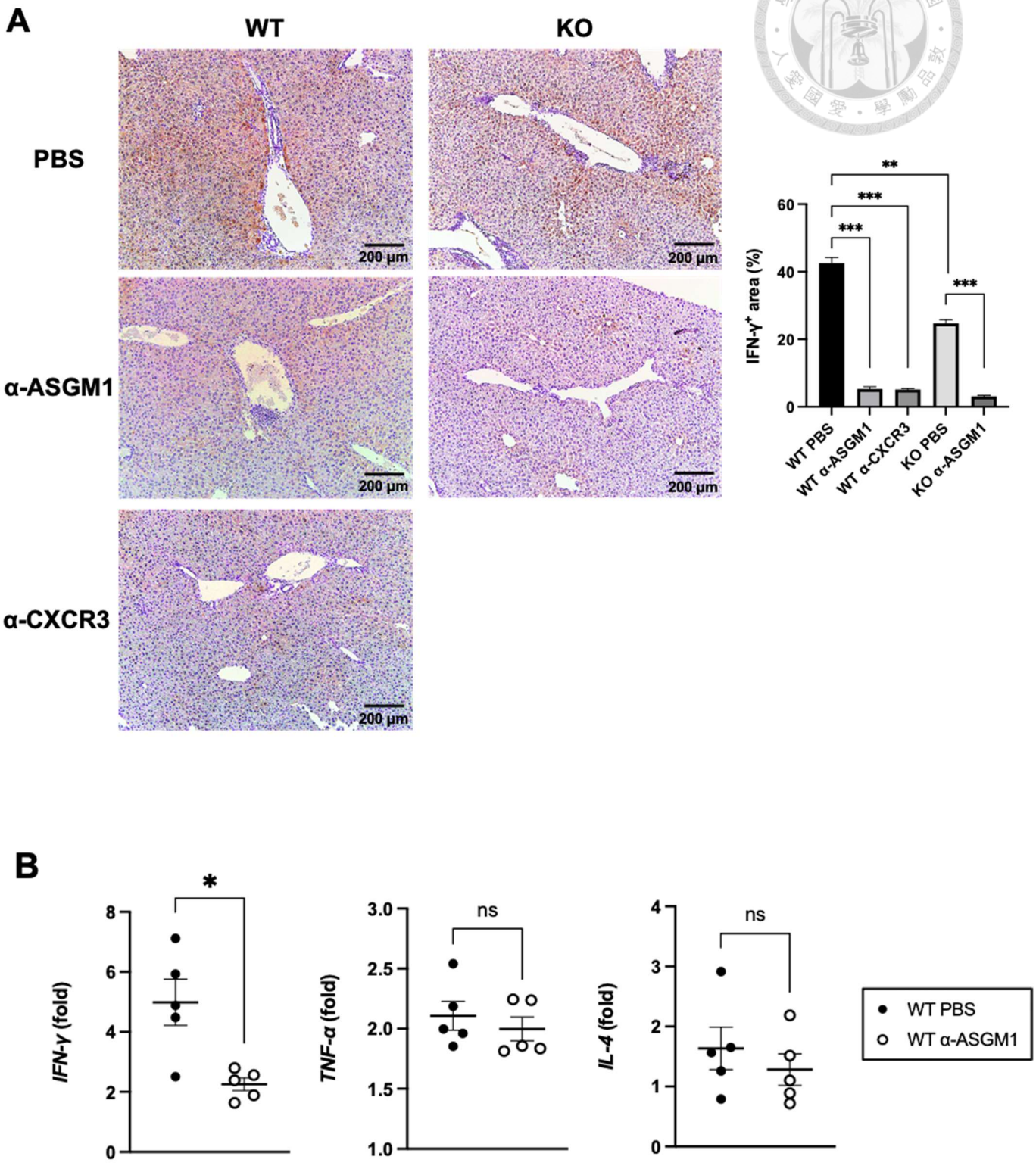

doi:10.6342/NTU202202017

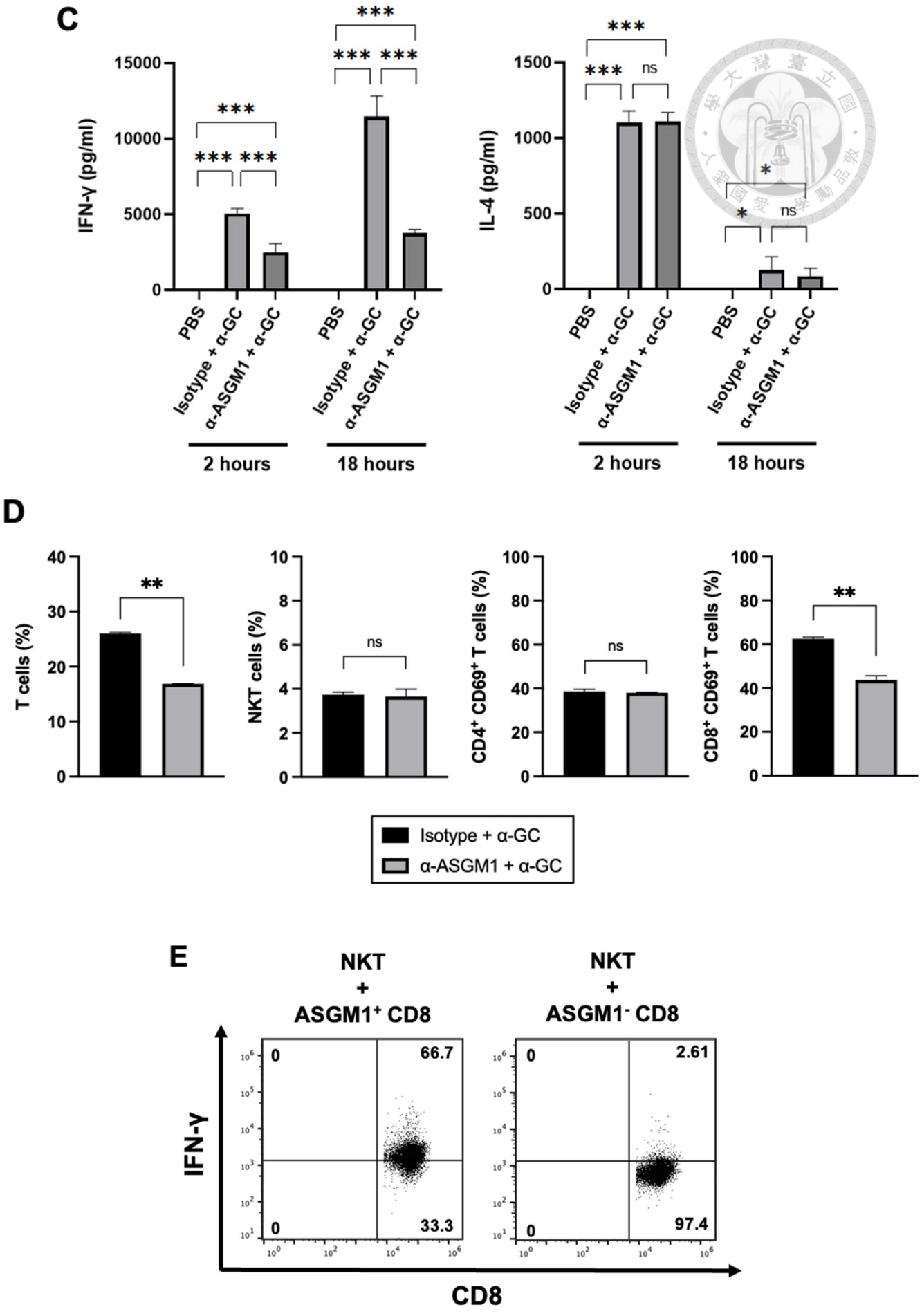

doi:10.6342/NTU202202017

Figure 6. α-GalCer-stimulated iNKT cells contributed to IFN-γ production by ASGM1$^+$ liver CD8$^+$ T cells in 2-OA-OVA immunized autoimmune cholangitis. (A) Representative immunohistochemical staining (× 100 magnification) of IFN-γ of liver sections. IFN-γ was stained brown, and the IFN-γ$^+$ area was analyzed by ImageJ software. (B) CD8 T cells were sorted from IHLs of PBC mice with/ without anti-ASGM1 treatment, and the expression levels of IFN-γ, TNF-α, and IL-4 mRNA in the liver were determined by RT-qPCR (C) α-GalCer (2 μg) was i.v. inducted, and α-ASGM1 was i.p. injected 24 hours before α-GalCer induction. Blood was acquired 2 hours and 18 hours post-α-GalCer induction. Serum levels of IFN-γ & IL-4 were detected by ELISA. (D) IHLs were harvested 24 hours post-α-GalCer induction. The percentage of total T, NKT, CD4$^+$ CD69$^+$, and CD8$^+$ CD69$^+$ cell populations were quantified by flow cytometry. (E) Naïve IHLs were sorted into ASGM1$^+$/ ASGM1$^-$ CD8 T cells and co-cultured with α-GalCer-stimulated NKT cells as a 1:1 ratio for 24 hours in 96-well flat-bottomed plates respectively. IFN-γ-producing CD8 T cells were determined by intracellular staining. Cells were pre-gated from CD3$^+$ NK1.1$^-$. *$p < 0.05$; **$p < 0.01$; ***$p < 0.001$ between selected relevant comparisons by Student's t-test or one-way ANOVA followed by Tukey multiple comparison test.

doi:10.6342/NTU202202017

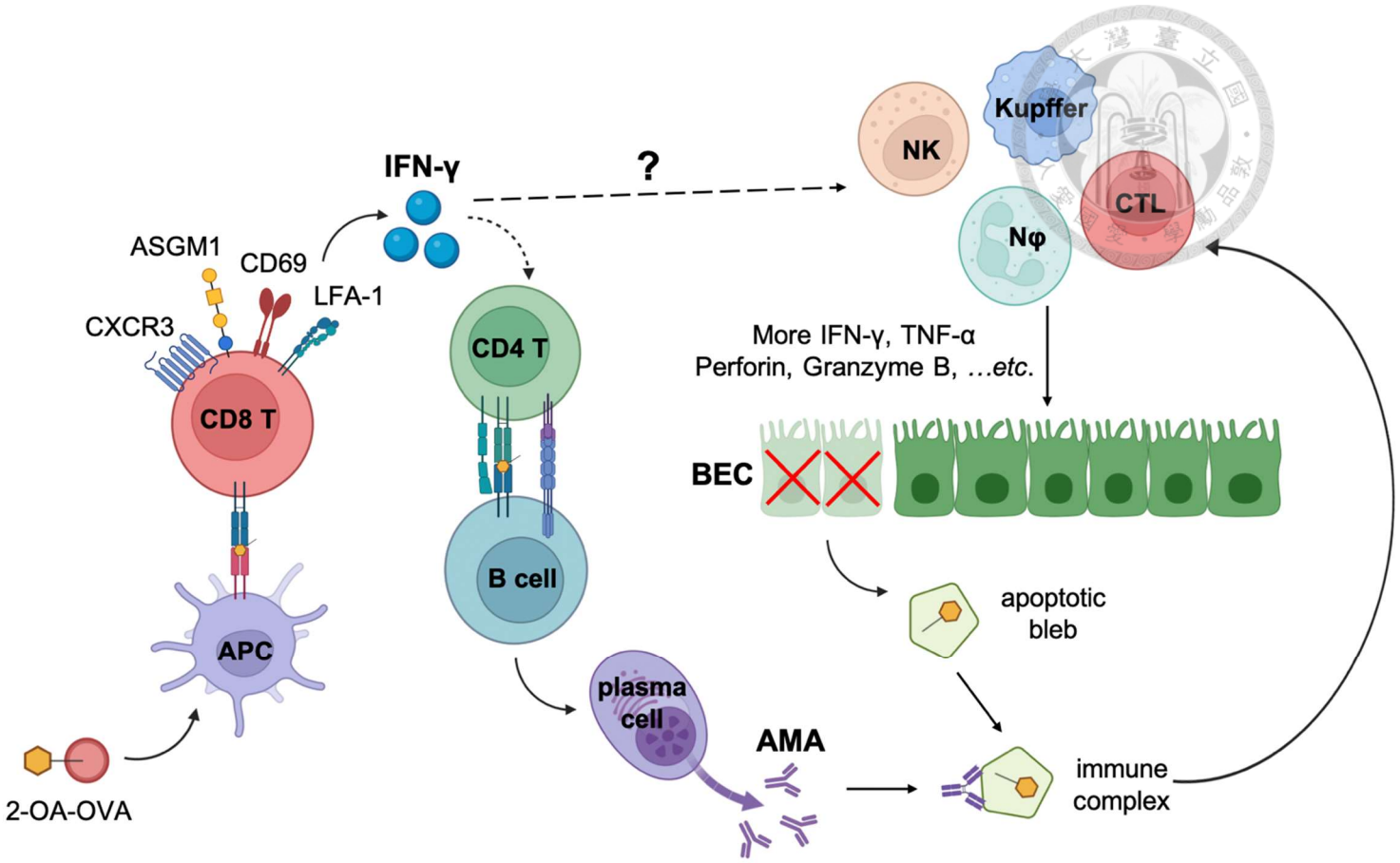

Figure 7. Graphical abstract of the working model. Under 2-OA-OVA immunized autoimmune cholangitis model, 2-OA-OVA presented by antigen-presenting cells (APC) activated ASGM1$^+$ CD8 T cells. By largely producing IFN-γ, ASGM1$^+$ CD8 T cells may contribute to the priming and activation of other effector lymphocytes to further induce apoptosis of biliary epithelial cells, autoantibody production, and ultimately exaggerate the autoimmune cholangitis. However, anti-ASGM1 treatment suppressed the 2-OA-OVA immunized autoimmune cholangitis through the depletion of IFN-γ-producing ASGM1$^+$ CD8 T cells.

doi:10.6342/NTU202202017

Chapter 6 References

1 Su, G. L. *et al.* Kupffer cell activation by lipopolysaccharide in rats: role for lipopolysaccharide binding protein and toll-like receptor 4. *Hepatology* **31**, 932-936, doi:10.1053/he.2000.5634 (2000).

2 Elsegood, C. L. *et al.* Kupffer cell-monocyte communication is essential for initiating murine liver progenitor cell-mediated liver regeneration. *Hepatology* **62**, 1272-1284, doi:10.1002/hep.27977 (2015).

3 Gabrilovich, D. I. & Nagaraj, S. Myeloid-derived suppressor cells as regulators of the immune system. *Nat Rev Immunol* **9**, 162-174, doi:10.1038/nri2506 (2009).

4 Doherty, D. G. *et al.* The human liver contains multiple populations of NK cells, T cells, and CD3+CD56+ natural T cells with distinct cytotoxic activities and Th1, Th2, and Th0 cytokine secretion patterns. *J Immunol* **163**, 2314-2321 (1999).

5 Kenna, T. *et al.* NKT cells from normal and tumor-bearing human livers are phenotypically and functionally distinct from murine NKT cells. *J Immunol* **171**, 1775-1779, doi:10.4049/jimmunol.171.4.1775 (2003).

6 Kenna, T. *et al.* Distinct subpopulations of gamma delta T cells are present in normal and tumor-bearing human liver. *Clin Immunol* **113**, 56-63, doi:10.1016/j.clim.2004.05.003 (2004).

7 Dusseaux, M. *et al.* Human MAIT cells are xenobiotic-resistant, tissue-targeted, CD161hi IL-17-secreting T cells. *Blood* **117**, 1250-1259, doi:10.1182/blood-2010-08-303339 (2011).

8 Racanelli, V. & Rehermann, B. The liver as an immunological organ. *Hepatology* **43**, S54-62, doi:10.1002/hep.21060 (2006).

9 Schenkel, J. M. & Masopust, D. Tissue-resident memory T cells. *Immunity* **41**, 886-897, doi:10.1016/j.immuni.2014.12.007 (2014).

10 Amsen, D., van Gisbergen, K., Hombrink, P. & van Lier, R. A. W. Tissue-resident memory T cells at the center of immunity to solid tumors. *Nat Immunol* **19**, 538-546, doi:10.1038/s41590-018-0114-2 (2018).

11 Bartsch, L. M., Damasio, M. P. S., Subudhi, S. & Drescher, H. K. Tissue-Resident Memory T Cells in the Liver-Unique Characteristics of Local Specialists. *Cells* **9**, doi:10.3390/cells9112457 (2020).

12 Fernandez-Ruiz, D. *et al.* Liver-Resident Memory CD8(+) T Cells Form a Front-Line Defense against Malaria Liver-Stage Infection. *Immunity* **45**, 889-902, doi:10.1016/j.immuni.2016.08.011 (2016).

13 Guidotti, L. G. *et al.* Immunosurveillance of the liver by intravascular effector CD8(+) T cells. *Cell* **161**, 486-500, doi:10.1016/j.cell.2015.03.005 (2015).

14 Warren, A. *et al.* T lymphocytes interact with hepatocytes through fenestrations in

doi:10.6342/NTU202202017

murine liver sinusoidal endothelial cells. *Hepatology* **44**, 1182-1190, doi:10.1002/hep.21378 (2006).

15 McNamara, H. A. *et al.* Up-regulation of LFA-1 allows liver-resident memory T cells to patrol and remain in the hepatic sinusoids. *Sci Immunol* **2**, doi:10.1126/sciimmunol.aaj1996 (2017).

16 Mackay, L. K. *et al.* Hobit and Blimp1 instruct a universal transcriptional program of tissue residency in lymphocytes. *Science* **352**, 459-463, doi:10.1126/science.aad2035 (2016).

17 Sung, C. C. *et al.* Asialo GM1-positive liver-resident CD8 T cells that express CD44 and LFA-1 are essential for immune clearance of hepatitis B virus. *Cell Mol Immunol* **18**, 1772-1782, doi:10.1038/s41423-020-0376-0 (2021).

18 Zhang, T., de Waard, A. A., Wuhrer, M. & Spaapen, R. M. The Role of Glycosphingolipids in Immune Cell Functions. *Front Immunol* **10**, 90, doi:10.3389/fimmu.2019.00090 (2019).

19 Bukowski, J. F., Woda, B. A., Habu, S., Okumura, K. & Welsh, R. M. Natural killer cell depletion enhances virus synthesis and virus-induced hepatitis in vivo. *J Immunol* **131**, 1531-1538 (1983).

20 Krawitt, E. L. Clinical features and management of autoimmune hepatitis. *World J Gastroenterol* **14**, 3301-3305, doi:10.3748/wjg.14.3301 (2008).

21 Sahebjam, F. & Vierling, J. M. Autoimmune hepatitis. *Front Med* **9**, 187-219, doi:10.1007/s11684-015-0386-y (2015).

22 Manns, M. P., Lohse, A. W. & Vergani, D. Autoimmune hepatitis--Update 2015. *J Hepatol* **62**, S100-111, doi:10.1016/j.jhep.2015.03.005 (2015).

23 Sucher, E. *et al.* Autoimmune Hepatitis-Immunologically Triggered Liver Pathogenesis-Diagnostic and Therapeutic Strategies. *J Immunol Res* **2019**, 9437043, doi:10.1155/2019/9437043 (2019).

24 Gulamhusein, A. F. & Hirschfield, G. M. Primary biliary cholangitis: pathogenesis and therapeutic opportunities. *Nat Rev Gastroenterol Hepatol* **17**, 93-110, doi:10.1038/s41575-019-0226-7 (2020).

25 Rodrigues, P. M. *et al.* Primary biliary cholangitis: A tale of epigenetically-induced secretory failure? *J Hepatol* **69**, 1371-1383, doi:10.1016/j.jhep.2018.08.020 (2018).

26 Younossi, Z. M. *et al.* Diagnosis and Management of Primary Biliary Cholangitis. *Am J Gastroenterol* **114**, 48-63, doi:10.1038/s41395-018-0390-3 (2019).

27 Hirschfield, G. M. & Gershwin, M. E. The immunobiology and pathophysiology of primary biliary cirrhosis. *Annu Rev Pathol* **8**, 303-330, doi:10.1146/annurev-pathol-020712-164014 (2013).

28 Chung, B. K. *et al.* Phenotyping and auto-antibody production by liver-infiltrating

doi:10.6342/NTU202202017

B cells in primary sclerosing cholangitis and primary biliary cholangitis. *J Autoimmun* **77**, 45-54, doi:10.1016/j.jaut.2016.10.003 (2017).

29 Katsumi, T. *et al.* Animal models of primary biliary cirrhosis. *Clin Rev Allergy Immunol* **48**, 142-153, doi:10.1007/s12016-015-8482-y (2015).

30 Wakabayashi, K. *et al.* Loss of tolerance in C57BL/6 mice to the autoantigen E2 subunit of pyruvate dehydrogenase by a xenobiotic with ensuing biliary ductular disease. *Hepatology* **48**, 531-540, doi:10.1002/hep.22390 (2008).

31 Shimoda, S. *et al.* The role of natural killer (NK) and NK T cells in the loss of tolerance in murine primary biliary cirrhosis. *Clinical & Experimental Immunology* **168**, 279-284, doi:10.1111/j.1365-2249.2012.04581.x (2012).

32 Wu, S. J. *et al.* Innate immunity and primary biliary cirrhosis: activated invariant natural killer T cells exacerbate murine autoimmune cholangitis and fibrosis. *Hepatology* **53**, 915-925, doi:10.1002/hep.24113 (2011).

33 Stark, R. *et al.* T RM maintenance is regulated by tissue damage via P2RX7. *Sci Immunol* **3**, doi:10.1126/sciimmunol.aau1022 (2018).

34 Zunder, E. R. *et al.* Palladium-based mass tag cell barcoding with a doublet-filtering scheme and single-cell deconvolution algorithm. *Nat Protoc* **10**, 316-333, doi:10.1038/nprot.2015.020 (2015).

35 Finck, R. *et al.* Normalization of mass cytometry data with bead standards. *Cytometry A* **83**, 483-494, doi:10.1002/cyto.a.22271 (2013).

36 Han, G. *et al.* Atomic mass tag of bismuth-209 for increasing the immunoassay multiplexing capacity of mass cytometry. *Cytometry A* **91**, 1150-1163, doi:10.1002/cyto.a.23283 (2017).

37 Wang, Y. & Zhang, C. The Roles of Liver-Resident Lymphocytes in Liver Diseases. *Front Immunol* **10**, 1582, doi:10.3389/fimmu.2019.01582 (2019).

38 Hsueh, Y. H. *et al.* Endogenous IL-10 maintains immune tolerance but IL-10 gene transfer exacerbates autoimmune cholangitis. *J Autoimmun* **95**, 159-170, doi:10.1016/j.jaut.2018.09.009 (2018).

39 Chang, C. H. *et al.* Innate immunity drives the initiation of a murine model of primary biliary cirrhosis. *PLoS One* **10**, e0121320, doi:10.1371/journal.pone.0121320 (2015).

40 Kamizono, S. *et al.* Nfil3/E4bp4 is required for the development and maturation of NK cells in vivo. *J Exp Med* **206**, 2977-2986, doi:10.1084/jem.20092176 (2009).

41 Harada, K. *et al.* In situ nucleic acid hybridization of cytokines in primary biliary cirrhosis: predominance of the Th1 subset. *Hepatology* **25**, 791-796, doi:10.1002/hep.510250402 (1997).

42 Kano, A., Watanabe, Y., Takeda, N., Aizawa, S. & Akaike, T. Analysis of IFN-

doi:10.6342/NTU202202017

gamma-induced cell cycle arrest and cell death in hepatocytes. *J Biochem* **121**, 677-683, doi:10.1093/oxfordjournals.jbchem.a021639 (1997).

43 Morita, M., Watanabe, Y. & Akaike, T. Protective effect of hepatocyte growth factor on interferon-gamma-induced cytotoxicity in mouse hepatocytes. *Hepatology* **21**, 1585-1593 (1995).

44 Constant, S. L. & Bottomly, K. Induction of Th1 and Th2 CD4+ T cell responses: the alternative approaches. *Annu Rev Immunol* **15**, 297-322, doi:10.1146/annurev.immunol.15.1.297 (1997).

45 Pellicci, D. G. *et al.* Differential recognition of CD1d-alpha-galactosyl ceramide by the V beta 8.2 and V beta 7 semi-invariant NKT T cell receptors. *Immunity* **31**, 47-59, doi:10.1016/j.immuni.2009.04.018 (2009).

46 Kosaka, A. *et al.* AsialoGM1+CD8+ central memory-type T cells in unimmunized mice as novel immunomodulator of IFN-gamma-dependent type 1 immunity. *Int Immunol* **19**, 249-256, doi:10.1093/intimm/dxl140 (2007).

47 You, Z. *et al.* The Clinical Significance of Hepatic CD69(+) CD103(+) CD8(+) Resident-Memory T Cells in Autoimmune Hepatitis. *Hepatology* **74**, 847-863, doi:10.1002/hep.31739 (2021).

48 Chuang, Y. H. *et al.* Increased killing activity and decreased cytokine production in NK cells in patients with primary biliary cirrhosis. *J Autoimmun* **26**, 232-240, doi:10.1016/j.jaut.2006.04.001 (2006).

49 Holz, L. E. *et al.* CD8(+) T Cell Activation Leads to Constitutive Formation of Liver Tissue-Resident Memory T Cells that Seed a Large and Flexible Niche in the Liver. *Cell Rep* **25**, 68-79 e64, doi:10.1016/j.celrep.2018.08.094 (2018).

doi:10.6342/NTU202202017